Title

Setting the curve: the biophysical properties of lipids in mitochondrial form and function.

Journal

Journal of Lipid Research, 65(10)

Authors

Venkatraman, Kailash
Lee, Christopher
Budin, Itay

Publication Date

2024-09-18

DOI

10.1016/j.jlr.2024.100643

Peer reviewed

JLR REVIEW

Setting the curve: the biophysical properties of lipids in mitochondrial form and function

Kailash Venkatraman[1], **Christopher T. Lee**[2], **and Itay Budin**[1]*

[1]Department of Chemistry and Biochemistry, and the [2]Department of Molecular Biology, University of California San Diego, La Jolla, CA, USA

Abstract Mitochondrial membranes are defined by their diverse functions, complex geometries, and unique lipidomes. In the inner mitochondrial membrane, highly curved membrane folds known as cristae house the electron transport chain and are the primary sites of cellular energy production. The outer mitochondrial membrane is flat by contrast, but is critical for the initiation and mediation of processes key to mitochondrial physiology: mitophagy, interorganelle contacts, fission and fusion dynamics, and metabolite transport. While the lipid composition of both the inner mitochondrial membrane and outer mitochondrial membrane have been characterized across a variety of cell types, a mechanistic understanding for how individual lipid classes contribute to mitochondrial structure and function remains nebulous. In this review, we address the biophysical properties of mitochondrial lipids and their related functional roles. We highlight the intrinsic curvature of the bulk mitochondrial phospholipid pool, with an emphasis on the nuances surrounding the mitochondrially-synthesized cardiolipin. We also outline emerging questions about other lipid classes — ether lipids, and sterols — with potential roles in mitochondrial physiology. We propose that further investigation is warranted to elucidate the specific properties of these lipids and their influence on mitochondrial architecture and function.

Supplementary key words phospholipids • mitochondria • cardiolipin • curvature • plasmalogens • sterols

Mitochondria are prime examples of the complexity and compositional diversity that define eukaryotic membranes. As double-membraned organelles, they contain an outer mitochondrial membrane (OMM) that envelopes an invaginated inner mitochondrial membrane (IMM). The OMM and IMM are functionally distinct. The IMM is the main site of ATP synthesis, with the electron transport chain (ETC) and ATP synthase complexes localized in inward folds of the IMM, known as cristae. The OMM predominantly acts as a diffusion barrier for metabolites, cations, and other molecules into and out of mitochondria (1–3), but more recently has been implicated in key processes regulating mitochondrial health, such as in mitophagy, fission/fusion, and maintenance of interorganelle contacts (4, 5). Corresponding to these differing functions, membrane lipid compositions of the OMM and IMM are significantly different, particularly in relative abundances of their phospholipid (PL) classes (6–9). Numerous studies have shown that the lipidomes of both membranes are tightly regulated, with defects associated with disease phenotypes where severe mitochondrial dysfunction is observed (10–13). Thus, the mechanisms by which lipids influence the structure and function of mitochondrial membranes is an active area of lipid research.

Both the metabolic functions of mitochondria and their dynamic cycles of fission and fusion depend on the formation of highly curved membrane topologies. A range of studies have demonstrated a direct relationship between curvature generation by cristae-shaping proteins, such as ATP synthase dimers and the mitochondrial contact site and cristae organization system complex, and the formation of highly curved, cristae membrane (CM) morphologies (**Fig. 1**) (14–18). Here, we focus on analogous roles for lipid-driven membrane curvature in contributing to mitochondrial structure and function (15, 19). Elucidation of lipid-mediated mechanisms for this organelle could explain the strict regulation of mitochondrial lipids and the significant phenotypes that arise when they are dysregulated in disease. To this end, we review models for how individual lipid and bulk membrane properties influence mitochondrial architecture and how biosynthetic adaptations of these lipids help to maintain membrane curvature under stressful conditions. We will begin by considering this phenomenon through the lens of spontaneous curvatures of mitochondrial PLs, but will extend our discussion to other lipid classes such as ether lipids and sterols, both of which have recently

*For correspondence: Itay Budin, ibudin@ucsd.edu.

https://doi.org/10.1016/j.jlr.2024.100643

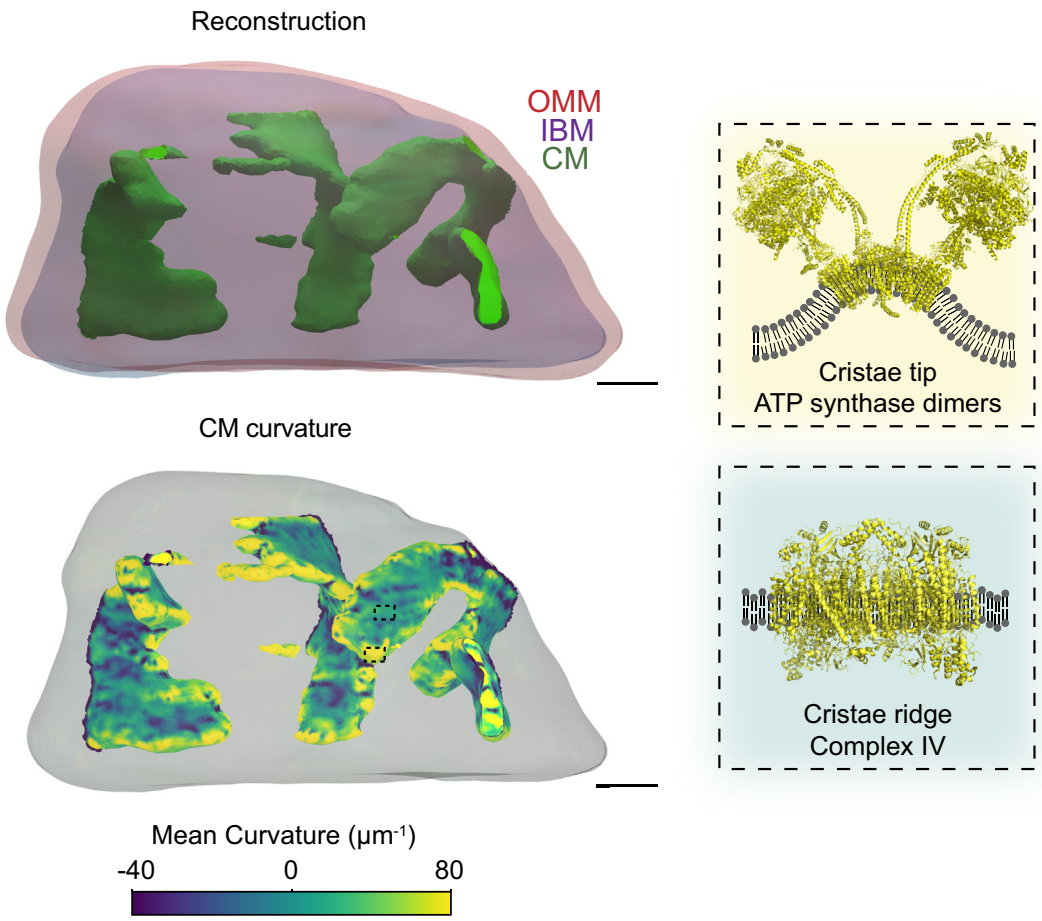

Fig. 1. Cristae are sites of membrane curvature in mitochondria. (A) Cristae membranes (CM) exhibit high curvature at cristae tips and cristae junctions as derived from curvature analysis using GAMer 2 software on 3D reconstructions of yeast mitochondrial membranes derived from multitilt electron tomography. The outer mitochondrial membrane (OMM) and inner boundary membrane (IBM) by contrast are flat, low curvature structures. The 3D reconstruction and GAMer 2 analysis pipeline was conducted as previously described (19, 22, 23). Scale bars, 50 nm. The formation of highly curved CMs predominantly occurs via membrane bending by cristae shaping proteins, such as ATP synthase dimers at the cristae tips, which form dense rows along CMs, and OPA1/MICOS at the cristae junctions. In contrast, the cristae ridges are flatter and house the key components of the ETC. Structures of the bovine ATP synthase dimer (PDB ID:7AJF) and bovine complex IV (PDB ID:1V54). ETC, electron transport chain; MICOS, mitochondrial contact site and cristae organization system; OPA1, optic atrophy protein 1.

been implicated in shaping mitochondrial structure and function under pathological conditions (20, 21).

MITOCHONDRIA ARE ENRICHED IN HIGH-CURVATURE, NONBILAYER PLs

The ability to isolate and analyze mitochondria from biological samples underlies our knowledge of its lipidome. Mitochondrial purification techniques were first developed in the 1930s (24) and isolation of intact mitochondria followed soon after (25–27). Since then, the isolation of pure, functional mitochondrial fractions from a variety of sources have become routine (7, 9, 28). Coupled with the advancement of LC-MS and LC-MS/MS and shotgun (MS/MS) lipidomics platforms, biochemical purification has allowed for accurate characterization of mitochondrial lipidomes from various tissues and organisms (29–33). Methods exist to biochemically separate OMM and IMM fractions of mitochondria (34, 35), which have been crucial in determining the subcellular localization of mitochondrial lipid-synthesizing enzymes (7), but also in elucidating submitochondrial lipid distribution (7, 9). These techniques have been powerful for defining mitochondrial lipidomes to a more detailed extent than most, if not all, other organelle membranes. It is important to note that mitochondrial isolation still yields some contaminants, especially lipids from closely apposed endoplasmic reticulum (ER) membranes. Similarly, pure mitoplast (IMM) or OMM isolations are also challenging (36). Improvements to mitochondrial isolation techniques have also been developed, allowing for purer fractionation and lipidome characterization (28, 37). Therefore, care must be taken when comparing mitochondrial lipidomes derived from different tissues, organisms or growth conditions, as these can affect potential impurities.

The most well-characterized and highly abundant components of the mitochondrial lipidome are its PLs. While the mitochondrial phospholipidome is significantly dependent on tissue and organism in mammals, its main constituents are largely conserved, even across eukaryotic phyla (7). The IMM primarily consists of phosphatidylcholine (PC), phosphatidylethanolamine (PE), and cardiolipin (CL), the latter of which is specifically synthesized and localized in the IMM alongside its precursor phosphatidylglycerol (PG). In comparison, the OMM consists of higher concentrations of PC and lower concentrations of PE, with only trace amounts of CL (9). In mammalian cells and plants, the OMM contains more phosphatidylinositol (PI) than the IMM, but in the yeast *Saccharomyces cerevisiae,* more PI is present in the IMM (8, 9). Other PLs such as phosphatidic acid (PA) and phosphatidylserine (PS), which are biosynthetic precursors of CL and PE, respectively, exist in lower concentrations in both the OMM and IMM (9). These PL classes are defined by the structure of their polar head groups, but can also feature distinctive fatty acyl chains that vary in length and number of double bonds (unsaturations).

A unique characteristic of the IMM is its enrichment in PLs whose structure promotes nonbilayer lipid phases (9). A lipid's intrinsic spontaneous curvature (c_0) describes its preferred geometric packing (38) and, as a simplified approximation, the shape of its average state in a relaxed membrane monolayer that is not under tension. Both lipid phases and c_0 values are generally measured using scattering techniques, such as small angle X-ray scattering (SAXS) (39). In SAXS experiments, lipids in suspension yield radially symmetrical scattering patterns, which can be averaged circumferentially to yield a scattering profile. PLs produce scattering patterns with concentric rings, which translate into profiles with distinct peaks. The spacing of these peaks can be used to identify the lipid mesophase and to determine some of its dimensions. The c_0 parameter has units of inverse length and is defined as the reciprocal of the radius of an unstressed lipid monolayer: low curvature ($c_0 \approx 0$) lipids, like PC, form flat, ordered monolayers that produce lamellar (L_α) phases (40), where lipids are organized into bilayers that form the basis of cell membrane structure (**Fig. 2**A). Negatively curved lipids ($c_0 < 0$) like PE, exhibit monolayers curved towards the head group and, in isolation, form nonlamellar phases; where lipid monolayers curl to form tubules that pack in a hexagonal array around water cores (Fig. 2A) (41, 42), termed the inverted hexagonal phase (H_{II}). Positively curved lipids ($c_0 > 0$) can also adopt nonlamellar lipid phases: at low lipid concentrations they can form micelles, with inward-facing hydrophobic cores and polar head groups facing outward, while at higher concentrations they tend to adopt hexagonal H_I phases (43).

The ability of lipids to form nonbilayer lipid mesophases is the basis for spontaneous curvature measurements (40, 41, 46, 47), as the radius of H_{II} tubules is used to calculate c_0. However, most lipids do not spontaneously form an H_{II} phase. They are thus included as "guests" in mixtures with a strongly H_{II}-forming lipid, like dioleoyl PE (DOPE). The change in H_{II} tubule radius that a guest lipid imparts versus a pure DOPE system can be used to determine its own c_0 value. Using this method, the curvatures of most major mitochondrial PLs have been measured (Fig. 2B): CL, PA, PS, and PG. CL and PA possess negative intrinsic curvatures, but milder than that of PE; PS exhibits positive c_0 values; and PG displays a near-zero c_0 (44, 48–51). A notable absence from this list is a curvature for PI, which has been observed to support the formation of nonlamellar cubic (Q) phases (52), and constitutes up to 15% and 5% of mitochondrial PLs in yeast and mammalian systems, respectively (9).

Spontaneous curvature measurements of individual PLs do have some important caveats. Measured curvature values are specific to the chemical environment in which they are measured. For example, the negative curvature of anionic lipids PA and CL is dependent on their ionic environment, as discussed further below (50, 53). Because they are carried out via measurement of H_{II} tubule diameter (Fig. 2A), measured c_0 values of most lipids take place in predominantly DOPE monolayers, a specific chemical environment that is very different from the distribution of lipids in real cell membranes. Extrapolation of these values to complex lipid bilayers in cells assumes a chemical mixing that is certainly not ideal. Nonetheless, trends in intrinsic membrane curvature can be imputed by general trends in the stoichiometry and relative curvatures of lipid components.

A long-standing question in lipid biology is why do cells produce so many nonbilayer lipids that can act against the stability of lamellar membranes. We (45) and others (54) have observed that organisms generally maintain the curvature of their lipidome, which can be extrapolated from the propensity of extracted lipids to transition from the L_α to H_{II} phase, in response to changes in the environment. We have defined net lipidome curvature as a weighted average of the c_0 value of all PLs based on their abundance. The maintenance of this parameter, termed homeocurvature adaptation, could act alongside homeoviscous adaptation, which maintains membrane fluidity (55), in dictating the regulation of lipid metabolism.

An intriguing hypothesis is that lipid transport processes act to maintain lipid curvature intracellularly in an organelle-specific manner. Compared to other organelles, mitochondria are particularly enriched in highly curved PE (9) and are the only subcellular location of nonbilayer-preferring CL. In mammals, measured mitochondrial PE/PC ratios (0.8) are higher than those of organelles such as the ER and Golgi (0.4) (9). The highly curved IMM also has nearly double the PE/PC ratio (1.15) than the relatively flat OMM (0.64)

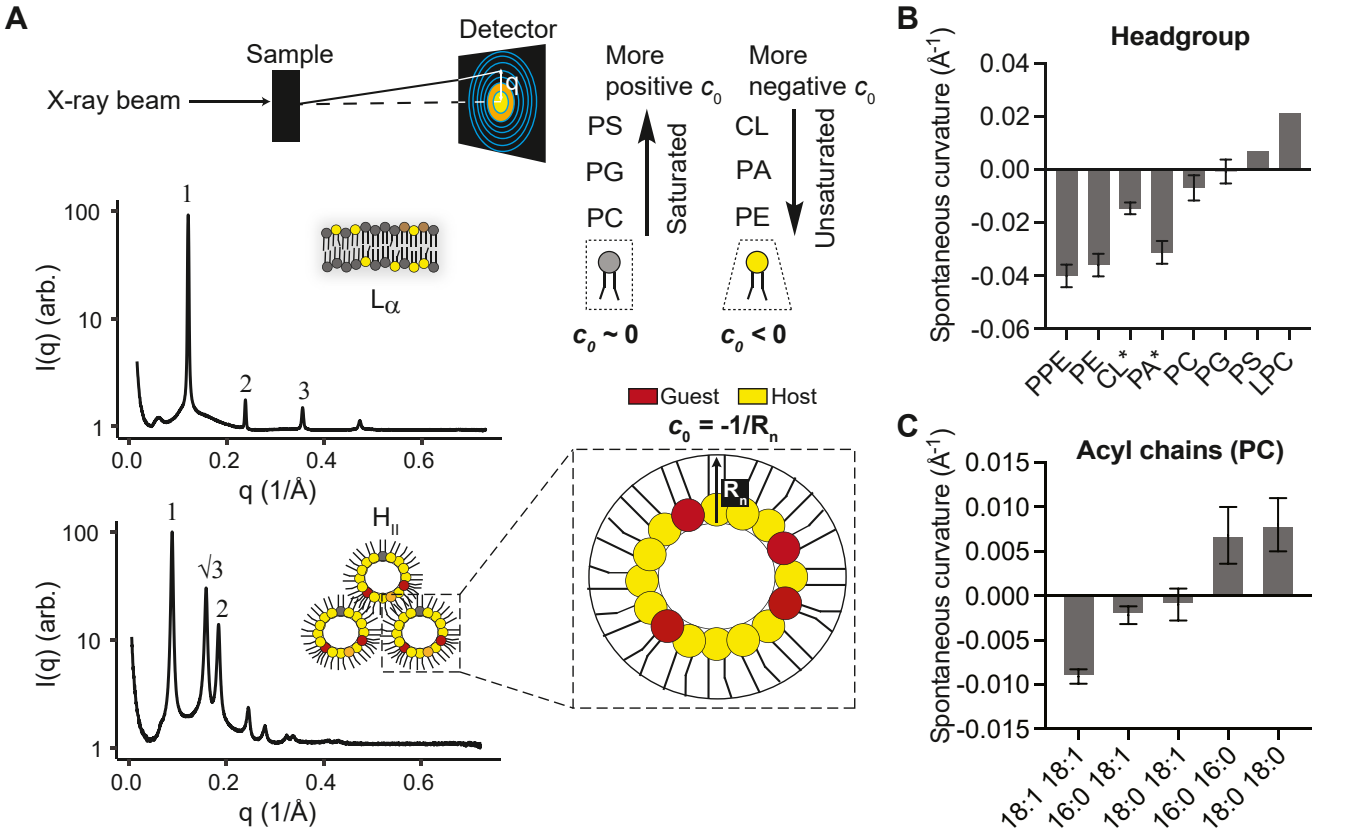

Fig. 2. Mitochondrial lipids and their SAXS-derived intrinsic curvatures. A: Shown is a schematic depiction of an X-ray scattering setup. The interference pattern on the detector can be used to determine the structures of lamellar (L_α) and inverted hexagonal (H_{II}) lipid phases from their corresponding SAXS intensity profiles. The distinctive Bragg peaks for each phase are noted. Spontaneous curvatures (c_0) of guest lipids (typically <20 mol %) are measured in hosted mixtures with DOPE. The radius of the neutral plane (R_n) is extracted from the peak location in the H_{II} scattering profile. The value of c_0 varies inversely with R_n ($c_0 = -1/R_n$). B: SAXS analysis has been performed on many mitochondrial PLs as hosted mixtures with DOPE. While tetra-oleoyl CL (TOCL) and dioleoyl PA (DOPA) exhibit negative curvatures in the presence of Ca^{2+} ions (*), PC and PG exhibit curvature values close to 0. Shown are curvatures of palmitoyl-oleoyl (PO) species, the most common species in mammalian cells. Di-oleoyl PS (DOPS) and lysolipids exhibit positive c_0 values. Plotted values of c_0 were acquired from SAXS analysis summarized in (44). Plasmenyl PE (PPE) c_0 values were reported in (45). C: Increasing levels of acyl chain saturation within a PL class drives c_0 values in the negative direction. Here, data for PC lipids analyzed in water is plotted. Values derived from (44). CL, cardiolipin; DOPE, dioleoyl phosphatidylethanolamine; PA, phosphatidic acid; PC, phosphatidylcholine; PE, phosphatidylethanolamine; PG, phosphatidylglycerol; PL, phospholipid; PS, phosphatidylserine; SAXS, small angle X-ray scattering.

(56), suggesting a particular preference of highly curved lipids. Given the predominance of unsaturated acyl chains, discussed further below, the IMM is thus specialized for large, negative lipid curvatures ("high-curvature lipids") compared to the rest of the cell.

How could lipid curvature translate to membrane curvature? High-curvature lipids do not necessarily impart any morphological effects on a bilayer if they are evenly distributed within and between both leaflets; in this case the curvature stress of each monolayer cancels out. Instead, lipids can act through mechanisms that are somewhat analogous to proteins that shape membrane curvature upon asymmetric binding, scaffolding, oligomerization, and crowding (57, 58). Firstly, the asymmetric distribution of curved lipids in the inner and outer leaflet of membranes can contribute to a curvature stress, which is balanced by net bending of a bilayer (**Fig. 3**). This may be particularly relevant for the IMM where CL is likely enriched in one IMM leaflet (59–61). Lateral heterogeneity or organization of high-curvature lipids on one leaflet can also be relevant for generating and supporting localized membrane curvature (62, 63) (Fig. 3), similar to BAR domain proteins (64) whose curvature generation depends on scaffolding. Measured enrichment of CL into high-curvature regions of liposomes undergoing deformation suggests such a phenomenon for this PL class, as discussed further below (65). Membrane curvature can also arise from the unbalanced distribution (number asymmetry) of lipids between leaflets (Fig. 3), which causes a differential stress between leaflets that can be alleviated by membrane bending, as has been described in the plasma membrane (66, 67). Such an imbalance could be relevant at sites at which PLs are transported from the ER, as well as through the activity of phospholipases (68), scramblases, and flippases (69).

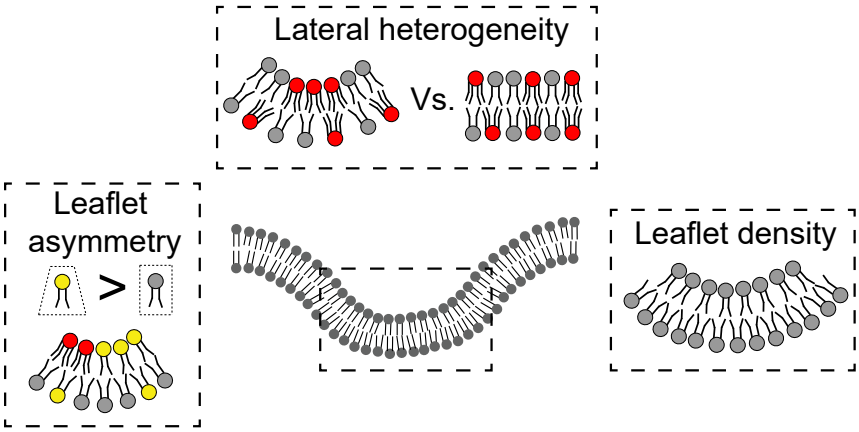

Fig. 3. Modalities of lipid-derived membrane curvature generation. The identification of the importance of membrane curvature in shaping cellular functions has necessitated analysis of pathways leading to curvature generation. Lipids can generate membrane curvature via 1) compositional differences between the two leaflets (leaflet asymmetry), for example, having more high-curvature lipids in the inner leaflet versus the outer leaflet. In the IMM, this could manifest as having more PE and CL compared to the outer leaflet 2) clustering of high-curvature lipids across a membrane (lateral heterogeneity), thus promoting local deformations and 3) an imbalance in the number of lipids (leaflet density) across a membrane, which drives surface area expansion of one leaflet leading to generation of curvature. CL, cardiolipin; IMM, inner mitochondrial membrane; PE, phosphatidylethanolamine.

Interestingly, a mitochondrial-localized scramblase, PL scramblase 3, has been identified to facilitate trans-IMM flipping of CL (70–72), while a recent study has also shown that OMM-localized VDAC1/2 can facilitate PL scrambling across the OMM (73).

All of these mechanisms can act alongside and be promoted by local deformations imposed by curvature-generating proteins. In particular, CL has been shown to cluster around deforming proteins (74), such as optic atrophy protein 1 (75), which could act together in contributing to IMM morphology. Nonbilayer lipids, especially CL, interact directly with many mitochondrial proteins and their complexes (18, 76–78) and could thus stabilize curvature-generating protein machinery. Lipid curvature is also thought to modulate the conformation and dynamics of membrane proteins, such as ion channels, through changes to the bilayer's lateral pressure profile and elasticity (79). While largely unexplored for mitochondrial proteins, this phenomenon could be especially relevant in the IMM given its enrichment in high-curvature lipids.

MITOCHONDRIAL PL METABOLISM PATHWAYS TO SUPPORT MEMBRANE ARCHITECTURE

Mitochondria synthesize a portion of the major cellular PLs within their membranes. Biosynthetic machinery for PE, CL, and PG are present within the IMM, while other PL classes, PC, PI, PA, and PS, are synthesized in the ER and then imported into mitochondria at contact sites and ER subfractions called mitochondrial associated membranes (**Fig. 4**) (71, 80, 81). While PE can also be synthesized in the ER through the cytidine diphosphate (CDP)-ethanolamine arm of the Kennedy pathway (82), the mitochondrial pool of PE is generated from the decarboxylation of imported PS by phosphatidylserine decarboxylase 1 (Psd1 in yeast, PISD in humans) in the IMM (Fig. 4) (81, 83–86). The synthesis of CL begins with delivery of PA from the OMM to the IMM via the Ups1-Mdm35 complex (yeast) or the TRIAP1/PRELI complex (human) (87–90), where it is converted to CDP diacylglycerol (CDP-DAG) by a CDP-DAG synthase, Tam41 (TAMM41 in humans) (91, 92). CDP-DAG is then converted into PG via PG phosphate by the sequential action of PG phosphate synthase and a protein tyrosine phosphatase, mitochondria 1 in humans, and Pgs1 and Gep4 in yeast (91, 93–95). Finally, CL synthase (Crd1 in yeast, CLS1 in mammals), generates CL through a condensation reaction between PG and CDP-DAG (Fig. 4) (96–98).

For both classes of mitochondrial produced PLs (CL and PE), the respective precursor PLs (PG and PS) are of milder curvature compared to their final biosynthetic products. Could this be a specific demand of the IMM for high-curvature lipids? In mice, loss of CL or mitochondrial PE leads to embryonic lethality (99, 100) and knockdown of PISD results in mitochondrial fragmentation and reduced respiration (101). Indeed, coordinated depletion of both CL and mitochondrial PE (via Psd1) in yeast has also been shown to be synthetically lethal (102), potentiating the idea of a specific requirement for negative lipid curvature within mitochondria. Both CL and PE have both been shown to interact with, and are required for optimal activity of major curvature-generating complexes in the IMM, such as ATP synthase and ETC super complexes (76–78, 103–105). However, loss of Crd1 or Psd1 in yeast does not perturb organization of ATP synthase (32, 104) nor does their absence cause significant changes to cristae ultrastructure under common growth conditions (32, 104). However, when yeast cells are grown microaerobically or genetically altered to increase saturated lipids, loss of

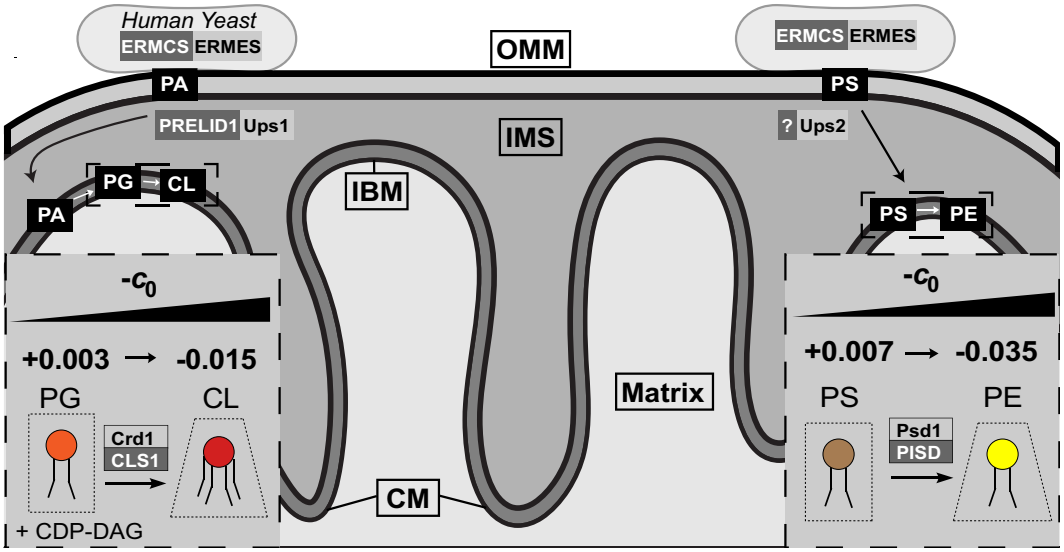

Fig. 4. Mitochondrial CL and PE biosynthesis occur in the direction of increasing negative curvature. CL and PE synthesis occurs in the mitochondria from imported precursors PA and PS respectively. For CL synthesis, PA is transferred from the OMM to the IMM by the TRIAP1-PRELID1 complex in humans and by Ups1-Mdm35 in yeast. In the IMM, it is then converted to PG by PG synthase and a PG phosphatase. PG is then converted to de novo CL by CL synthase. For PE synthesis, imported PS is transferred from the OMM to IMM by Ups2 in yeast and by an unidentified mechanism in humans. PS is then decarboxylated into PE by PISD in humans and Psd1 in yeast. The magnitude of intrinsic curvatures for CL and PE (in $Å^{-1}$) are higher than their respective precursors, suggesting that mitochondrial lipid metabolism corresponds to increasing negative lipidome curvature in the IMM. CL, cardiolipin; IMM, inner mitochondrial membrane; OMM, outer mitochondrial membrane; PA, phosphatidic acid; PE, phosphatidylethanolamine; PG, phosphatidylglycerol; PS, phosphatidylserine.

Crd1 causes the collapse of CMs, leaving cells with a flat IMM and mitochondria lacking respiratory capacity (19).

ACYL CHAIN HOMEOSTASIS IN MITOCHONDRIAL PLs

Canonically, the acyl chain composition (length and unsaturation) of PLs regulates their fluidity (106). Increasing the abundance of unsaturated lipids has been shown to increase membrane fluidity and concomitantly respiration (107), potentially by speeding of diffusion coupled reactions in the ETC (108). Less appreciated than its effect on membrane fluidity, acyl chain composition also impacts the intrinsic curvatures of lipids. Numerous scattering-based studies, predominantly on PC and PE lipids, have demonstrated that changing the length and unsaturation of PLs alter their H_{II} transition temperatures and c_0 values (Fig. 2C) (109, 110). In general, more unsaturated acyl chains decrease c_0 and cause PLs to undergo H_{II} transitions at lower temperatures (110) due to the increased volume of highly disordered acyl chains. This is especially the case for PLs that contain long polyunsaturated fatty acids (111).

Although head group heterogeneity within cells is well characterized, emerging evidence suggests that mitochondrial membranes are also defined by a high degree of acyl chain unsaturation. In yeast, mitochondria are particularly enriched in unsaturated PLs in comparison to the whole cell (7), and contain very low levels of saturated PLs, even upon genetic inhibition of desaturases (19). PLs containing disaturated acyl chains can form lamellar gel (L_β) phases in the absence of sterols (110, 112), which could be especially disruptive in mitochondria due to their leakiness and reduced dynamics. One mechanism for this selectivity is an import preference of unsaturated PLs, particularly PS for PE synthesis, from ER to mitochondria at membrane contact sites (113). The preferential import and decarboxylation of unsaturated PS as a substrate for PE synthesis has been observed in yeast and mammalian cells (113–115). In addition, compared to other organelles, mitochondria are buffered against changes to membrane fluidity imposed by exogenous treatment with saturated fatty acids (SFAs), implying mechanisms preventing the accumulation of saturated lipids in the mitochondria (116).

The exogenous addition of SFAs is a common model for metabolic disorders and results in mitochondrial dysfunction and cytochrome *c* release in cell culture (117, 118). Mice and rats fed a diet high in SFAs also show reduced respiratory capacity and increased reactive oxygen species (ROS) production (119–121). Mitochondrial dysfunction is a hallmark of pathologies such as nonalcoholic fatty liver disease and obesity, where excessive SFAs lead to progression of the disease (122–124). Despite the breadth of these studies, the specific mechanisms governing the effects of SFA accumulation in mitochondria and subsequent lipidic adaptations have remained debated. Using a set of yeast strains that feature genetically controlled desaturate

activities, we found that a critical saturation level in mitochondria causes respiration loss through disassembly of ATP synthase dimers and oligomers (19). While cells generally compensated for increased saturation by decreasing the PE/PC ratio, we observed the opposite trend in the mitochondrion, a major increase in the PE/PC ratio. This change is counter to the maintenance of membrane fluidity, because PE has a higher melting temperature than PC. Instead, it acts to increase lipidome negative curvature (**Fig. 5**), potentially to compensate for loss of ATP synthase oligomers that shape CM ridges.

While numerous studies have demonstrated a significance for the cellular PE/PC ratio in maintaining membrane fluidity in disease conditions (125–127), specific changes to this ratio in mitochondria have been less well-investigated. One particularly intriguing study demonstrated that the loss of PE *N*-methyltransferase in mice, which is responsible for production of 30% hepatic PC, increased resistance to high-fat diet–induced obesity (128). The authors ascribed this phenomenon to increased mitochondrial PE and decreased mitochondrial PC, leading to increased respiratory capacity in PE N-methyltransferase$^{-/-}$ mice. These results exemplify a specific mitochondrial requirement for high-curvature PE over PC lipids. Mitochondrial-related phenotypes have frequently been observed in several disease conditions (e.g., nonalcoholic fatty liver disease, obesity, and diabetes mellitus type 2) (129–132), but the specific changes and regulation of mitochondrial PE/PC and subsequent effects on mitochondrial performance still remains to be elucidated. Mitochondrial-specific lipidomic analysis in lipid-driven disease states could be important for further unraveling PL homeostasis under metabolic stress.

OUTSTANDING QUESTIONS ABOUT CL CURVATURE

Unlike all other PLs, CL contains two phosphates in its head group linked by a glycerol bridge and has four acyl chains (133). The difference in cross-sectional area between the polar head and hydrophobic tails was long proposed to give rise to a conical-like structure with a negative c_0. However, the specifics of CL curvature remain contentious. One previous area of controversy is the ionization state of CL. Early work using pH titration experiments supported the model that the two phosphodiester groups of CL exhibited disparate pKa values, thus favoring the formation of the monoanionic form at physiological pH (134, 135), this model is

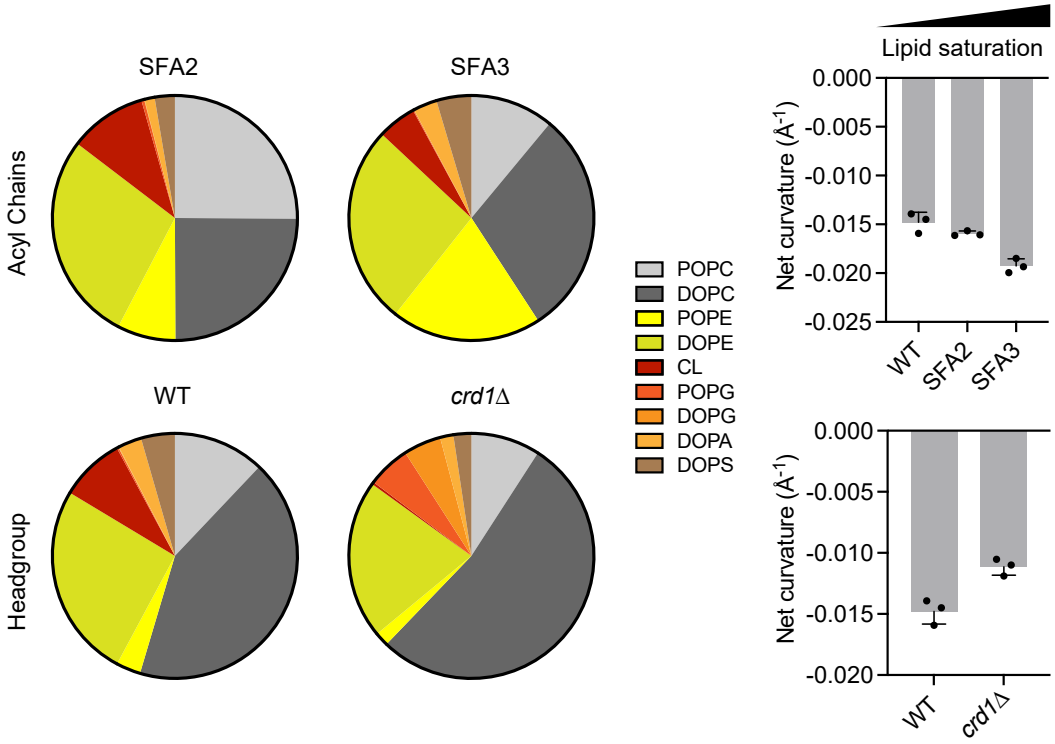

Fig. 5. Lipid metabolism mutants show spontaneous curvature adaptations in mitochondria. Tuning of PL saturation through manipulation of desaturase expression generated yeast strains designated as saturated fatty acid (SFA) with progressively increasing levels of SFAs. In isolated mitochondria from each strain, we observe increased levels of PE and reduced PC. This increase in PE results in increased magnitude of curvature (top). Other perturbations, such loss of CL through genetic deletion of CL synthase (*crd1*Δ), results in milder extrapolated lipidome curvature (bottom). Here, net curvature is defined as the average of c_0 values of all PLs weighted to their abundance. For calculation of net curvature, only lipids with c_0 from similar SAXS measurements were utilized (44). Lipidomic analysis was conducted on isolated mitochondria from yeast strains as described in (19). CL, cardiolipin; PC, phosphatidylcholine; PE, phosphatidylethanolamine; PG, phosphatidylglycerol; PL, phospholipid; SAXS, small angle X-ray scattering.

attractive due to its suggestion of the proton-trapping capabilities of the CL head group, implying a basis for its interaction with ETC components (136). However, more recent studies have definitively demonstrated that both phosphate groups exhibit strong dibasic acid characteristics with similarly low pKa values, thus favoring CL's dianionic behavior at physiological pH (137–140). This is relevant to the curvature properties of CL as the mono and dianionic forms of CL would have different intrinsic curvature properties, given the reduced charge repulsion of the former. Multiple studies have demonstrated that the packing of CL is significantly affected by pH (141–143), which may be relevant for influencing its curvature properties in locally acidic environments of the intermembrane space.

In bacterial membranes, CL localizes to higher curvature pole regions (144–146). Similarly, CL enriches in nanotubes derived from giant unilamellar vesicles generated by micropipette aspiration (65); extrapolation of intrinsic curvature from these experiments yielded a large magnitude value (-0.11 Å^{-1}) consistent with curvature-based sorting and clustering of CL. However, measurement of the spontaneous curvature of tetra-oleoyl CL in water using SAXS shows a c_0 close to zero (50). A stepwise increase of Ca^{2+} concentration results in nonlamellar properties and more negative values of c_0 (50, 53, 112, 147), although still milder than those for DOPE (44). Interestingly, Ca^{2+} levels have been shown to influence CL shape in pure lipid systems, but not in binary mixtures with PC (148, 149). Recent molecular dynamics (MD) simulations on mitochondrial model membranes suggest that CL curvature is dependent on the counterion distribution of H_3O^+, implying its dependence on the electrochemical environment surrounding CL (150). Numerous pathologies exhibit changes in mitochondrial levels of Ca^{2+}, largely due to mitochondrial permeability transition pore opening (151, 152) or dysfunction to the mitochondrial calcium uniporter (153, 154), however, the direct effect of altered Ca^{2+} on CL abundance and IMM composition has yet to be established.

One caveat with spontaneous curvature measurements is that the collective behavior of multiple lipids within a bilayer might not be captured as hosted mixtures in the H_{II} phase. The clustering of CL into areas of high-curvature experimentally, described above, and in MD simulations have demonstrated its curvature-dependent partitioning (19, 146, 155). These results suggest that the spatial organization of CL could be relevant for understanding its interplay with membrane curvature in the IMM. An additional factor contributing to CL function could be its asymmetric distribution across the IMM. Experimental evidence using inverted IMM vesicles and measurements with the CL-binding dye nonyl acridine orange have produced disparate results, with some studies suggesting an enrichment of CL in the outer (intermembrane space–facing) leaflet of the IMM (59, 60, 156), while others propose its enrichment to be on the inner (matrix-facing) leaflet (157). However, nonyl acridine orange binding could be nonspecific (158) and experiments measuring asymmetry of lipids like CL are inherently challenging. CL biosynthesis occurs on the inner leaflet of the IMM (159), but its remodeling by Tafazzin that is discussed further below, has been shown to occur on the outer leaflet of the IMM (160–162). Indeed, the leaflet distribution of CL may be dynamic and change in response to mitochondrial stress. Therefore, understanding the stimuli-driven changes in CL distribution may also be valuable to understanding mitochondrial lipid remodeling in disease states.

Above, we stipulated that the biosynthesis of mitochondrial lipids follows a general pattern of increasing intrinsic curvature. Another example of this phenomenon is in the remodeling process of CL acyl chains, which occurs exclusively in the IMM. De novo CL synthesized from the condensation of CDP-DAG and PG contains more saturated acyl chains compared to remodeled CL, so remodeled CL has a larger negative spontaneous curvature than de novo synthesized CL (32, 163). This nascent CL is then deacylated by a phospholipase A_2 (PLA_2) enzyme into monolysocardiolipin (MLCL), a 3-chained CL (164). Numerous enzymes with PLA_2 activity conduct this reaction in mammalian cells, but only Cld1 has been shown to deacylate CL in yeast (165). A transacylase known as tafazzin transfers an unsaturated acyl chain from PC to MLCL to form remodeled, unsaturated CL (166–168). Importantly, nonbilayer lipid environments promote Tafazzin activity (166), indicating a potential feedback loop for increasing lipid curvature in the IMM via CL remodeling. In the heart, the CL acyl chain composition is extremely tightly regulated, with linoleic acid (18:2) making up ~80% of CL acyl chains (169). Interestingly, the predominant acyl chain identity of CL is significantly dependent on tissue, with oleic acid (18:1) being more common in the colon and duodenum (169), while the brain exhibits a wider range of CL acyl chain identities (170). Regardless of some variations in acyl chain composition across tissues, CL generally contains unsaturation(s) on each acyl chain, a phenomenon also conserved in other organisms such as plants and yeast (171, 172). This is in contrast with other PLs, which typically feature a saturated *sn*-1 chain.

Dysregulation of CL acyl chain composition has been observed in several pathologies (173–175) the most famous of which is Barth syndrome (BTHS), a rare X-linked disease caused by mutations in *TAFAZZIN*, which manifests predominantly as cardiomyopathy, skeletal myopathy as well as neutropenia (11, 176–178). Notably, BTHS patients exhibit significantly aberrant cristae morphologies, providing early evidence of the specific requirement of CL for shaping IMM structure (179, 180). Lipidomic evidence has shown that BTHS patients

have reduced CL levels in addition to increases in MLCL and saturated nascent CL (181–184). Numerous studies across several model systems have observed elevated MLCL levels upon *TAFAZZIN* mutation (185–188), and that its presence negatively impacts ETC organization and respiration (187, 189, 190). However, mitigating the MLCL:CL ratio through treatment with the $iPLA_2$ inhibitor bromoenol lactone still results in reduced respiratory capacity, despite rescue of ETC organization (185, 191). This suggests that the presence of more saturated nascent CL or reduced CL levels themselves may still cause significant mitochondrial dysfunction independently of MLCL. We have observed that under conditions of increased lipid saturation, loss of CL deacylation by PLA_2 deletion in yeast (Cld1) or inhibition in HEK293 ($iPLA_2$) cells results in mitochondrial dysfunction (192), suggesting that the lipid environment may directly impact the interplay between CL remodeling and mitochondrial function even in low MLCL:CL conditions.

One explanation for a lack of mitochondrial rescue in BTHS cells with ameliorated MLCL:CL ratios could lie in the relative properties of MLCL and nascent CL compared to mature CL. While an experimental measurement of c_0 from MLCL is lacking, SAXS and NMR studies have demonstrated that MLCL has greater preference for the L_α phase compared to tetra-unsaturated CL (193, 194). Further, coarse-grained MD simulations have estimated a small positive c_0 for MLCL (195). Indeed, a recent study has demonstrated by a combination of cryogenic electron microscopy and MD analysis that the reduced curvature of MLCL compared to remodeled CL restricts the membrane remodeling capabilities of optic atrophy protein 1 (75), which may be a significant contributor to cristae deformation in BTHS. By comparison, X-ray diffraction analysis of fully saturated CL molecules has been conducted for tetrapalmitoyl-cardiolipin, $(16{:}0)_4$) and tetramyristoyl-cardiolipin $(14{:}0)_4$) (112, 196). Both tetramyristoyl-cardiolipin and tetrapalmitoyl-cardiolipin have high melting temperatures and exhibit gel phase characteristics at physiological temperatures, although a c_0 value has yet to be extracted from hosted mixtures in PE. Indeed, while no fully saturated CL molecules have been observed in BTHS patients, an increase in partially saturated palmitoyl-oleoyl CL ($16{:}0_2 18{:}1_2$) has been found (184). Therefore, biophysical measurements of MLCL and palmitoyl-oleoyl CL may be informative. In addition, studies on the morphological and respiratory defects caused by more saturated CL molecules separately from those of MLCL could be important in untangling some of the mechanisms underlying BTHS pathologies.

In addition to altered CL compositions in BTHS, more recent studies have shown that changing CL levels has been implicated as a marker of aging (94, 197, 198). However, conflicting effects have been observed with a dependency on tissue. In aged skeletal muscle mitochondria of mice, a significant increase in highly unsaturated CL content was observed (33). On the other hand, several studies have reported decreases in CL content in brain mitochondria of aged mice (198–202) and in rat hearts (203–206). CL synthesis or degradation thus appears to be correlated with lifespan. In the fungus *Podospora anserina*, loss of CL synthase markedly affects culture survivability (207). Similarly, ablation of CL levels in *S. cerevisiae* (through removal of Pgs1 or Crd1) resulted in reduced longevity, further implicating CL's crucial role in aged cells (208). A common explanation for these observed changes in longevity and reduction in CL content is through increased CL peroxidation (94, 209, 210), and notably, observed reductions in linoleic acid (18:2) incorporation into CL in aged rat hearts are coupled with increases in docosahexaenoic acid (22:6) and arachidonic acid (20:4), which are peroxidizable fatty acyl chains (211). However, other mechanisms, such as ETC dysfunction, cytochrome *c* release, and alterations to the mitochondrial bilayer independent of CL peroxidation may also be a consequence of reduced CL and altered CL composition in aged cells (173). Indeed, in a *P. anserina* model of aging, supplementation of linoleic acid was essential to maintaining the longevity phenotype of mitochondrial contact site and cristae organization system–depleted cells in the absence of CL remodeling (212). Furthermore, results in *S. cerevisiae*, which does not metabolize polyunsaturated fatty acids, also demonstrate a reduction in cell viability in conditions of altered CL metabolism, suggesting a possible peroxidation-independent mechanism (94, 208). Despite these interesting observations, a definitive mechanism by which CL reduction occurs and the general role of CL in bulk mitochondrial membrane properties in aging remains mysterious.

Numerous recent studies in cancer biology have also found unique adaptations of CL abundance and acyl chain composition in tumor tissue (213). The relative changes between CL seem to be tissue-specific. Decreases in CL abundance have been observed in subcutaneously grown brain tumors in mice (214) and in liver tumors (215), while a concomitant increase in the saturation of CL species was exhibited in the latter. More surprisingly, increases in CL have been observed in thyroid and liver tumors (216, 217) as well as in mitochondrial lipid extracts of human pancreatic and colon cancers (218). While specific analysis of mitochondrial lipidomes in cancer are rare, studies on patient hepatoma mitochondria have shown an increase in acyl chain saturation (219) and a major increase in the cholesterol:PL ratio (220), implying increased membrane rigidity. In hepatoma mitochondrial extracts, a decrease in CL was commonly observed (219, 221), however a concomitant increase in mitochondrial PE levels suggests a possible adaptation to curvature homeostasis. The large observed increase in CL content in colon cancer may be somewhat related to a unique relationship between CL, oxygen, and lipid saturation.

The colon contains lower O_2 levels than highly oxygenated tissues such as the heart and lung (222). Reduced oxygenation alters cellular lipid composition through inhibition of stearoyl-CoA desaturase 1 activity, resulting in an accumulation of SFAs (223, 224). Indeed, the essentiality of CL synthesis in low oxygen fitness has been shown in a recent genome-wide screen of intestinal T-cells (225). It is important to note the differences in SFA levels and ETC activities in cultured cells and tissues (226, 227), which may differentially affect glycolytic and respiratory metabolic rates as a result of glucose availability, as delineated by the crabtree effect (228, 229). These metabolic differences should be considered when analyzing lipidic changes from cell culture and tissues.

Our group has used yeast cells under low oxygen as a model for mitochondrial adaptations to increases in saturated lipids (19, 192). Natural yeast fermentation conditions are microaerobic and laboratory strains thrive under such conditions when provided glucose. Microaerobic yeast feature higher levels of saturated acyl chains across the entire lipidome, featuring PLs with predominantly saturated *sn*-1 chains, as in mammalian cells. This is in contrast to yeast grown under high laboratory aeration, which feature unsaturated *sn*-1 and *sn*-2 chains. Somewhat surprisingly, low oxygen growth drives a major expansion in the yeast IMM, leading to the formation of sheet-like CMs that also better mimic those observed in mammalian cells. Under these conditions, we observed a major (>2-fold) increase in CL levels and the expression of the CL remodeling pathway (19). Both CL synthesis and remodeling pathways are essential for CM ultrastructure under microaerobic growth, in contrast to highly aerated conditions where their loss yields more subtle phenotypes (32). Notably, increases in CL under microaerobic growth do not correspond to increases in ETC complexes, which are downregulated due to lack of oxidative phosphorylation, arguing against a sole function of CL in stabilizing mitochondrial protein complexes. These results suggest that the synthesis and remodeling of CL, which supports its biophysical properties, is required to maintain the morphology of the IMM in a manner that is dependent on the surrounding lipidome.

UNEXPLORED FUNCTIONS FOR EMERGING LIPID CLASSES IN THE MITOCHONDRION

While glycerophospholipids like PC, PE, and CL make up the bulk of the mitochondrial lipidome, roles for other lipid classes could become emerging areas of mitochondrial research. We highlight two lipid classes: 1) ether-linked PLs termed plasmalogens and 2) cholesterol and other sterols, as components that could strongly influence mitochondrial membrane properties and have established connections with human diseases.

Unearthing the role of ether lipid metabolism in health and disease is a rapidly emerging area of lipid biology. Plasmalogens are PLs that contain an alkenyl ether, often referred to as a vinyl ether, linkage at the *sn*-1 position, in contrast to the ester linkages found in canonical PLs (230–232). Plasmalogens can make up 15% of cellular PLs and are particularly enriched in the brain, but are also found to lesser extents in the heart, skeletal muscle, and liver (233). Plasmenyl PE (PPE) species predominate in the brain and are specifically enriched in the frontal and parietal cortices (233). On the other hand, ether-linked PC species are comparatively scarce in the brain but are present in larger quantities in heart and skeletal muscle (233). The first steps of plasmalogen biosynthesis from dihydroxyacetone phosphate, (DHAP) occur in peroxisomes, while the reduction of 1-alkyl DHAP is catalyzed by an alkyl DHAP reductase that is found in both peroxisomes and ER. The remaining steps of plasmalogen synthesis resemble glycero-PC and PE synthesis and occur in the ER (234), with the notable exception of the last step in their synthesis: the introduction of the vinyl ether unsaturation via the ER desaturase TMEM189 (235).

Plasmalogens have been reported to be bulk components of mitochondrial membranes but measurements of their abundances have yielded conflicting results. PPE has been reported to comprise as high as 40% (236), or as low as 10% (237) of the total mitochondrial PE pool. Similarly, one study reported plasmenyl PC to make up 20% of the mitochondrial PC pool (236), while another study using brown adipose tissue mitochondria from mice observed undetectable levels (237). Importantly, these studies were conducted on isolated mitochondria from different sources, and plasmalogen levels vary significantly between tissues (233), and thus may lead to significant variation in reported mitochondrial plasmalogen lipidomes. Lipidomic characterization of plasmalogens is also challenging due to their instability and associated difficulties in their handling and quantification. Therefore, additional careful studies are required to elucidate their subcellular distributions. The transport mechanisms of ether lipids are also unexplored, so it is unclear by what mechanism they could enter mitochondria. This is a key question, because plasmalogens have been proposed to serve as antioxidants, an effective sink for mitochondrial-generated ROS, and thus as potential regulators of lipid peroxidation (233, 238). This dynamic could underlie their emerging roles in ferroptosis (239). The oxidation-prone vinyl ether linkage could also explain why decreases in plasmalogen levels have been correlated with inflammation, neuropathology, and aging (233, 240, 241).

The vinyl ether linkage bequeaths plasmalogens with unique biophysical properties that have received less attention, yet could be especially relevant for the IMM. PPE membranes show a reduced L_α to H_{II} transition temperature compared to diacyl PE (242–244), implying

a higher propensity to form nonlamellar structures. Analysis of extracted lipids from plasmalogen-deficient strains of *Megasphaera elsdenii*, a common bacterium of the intestinal tract, showed no L_α to H_{II} transition in a temperature sweep up to 95°C, while plasmalogen-containing strains began to exhibit a transition after 50° C (245). Similarly, introduction of PPE biosynthesis into *Escherichia coli* cells causes a decrease in the L_α to H_{II} transition temperature (45). The nature of PPE's promotion of nonlamellar phases is still an open question. Based on early analyses of the PPE H_{II} phase, the vinyl ether linkage on the *sn*-1 position was suggested to contribute to minimizing the interstitial region between hydrophobic chains H_{II} tubules, which relieves the energetic cost of packing these chains, similar to the capacity of bulky hydrophobic molecules (tricosene and tetradecane) to act as relaxants (246). However, these analyses were performed on extracted PPE with varying acyl chain compositions. More recently, our group found that synthetic PPE has in fact a larger negative c_0 than diacyl PE, consistent with its high H_{II} propensity. PPE thus features the highest curvature of any PL class (45). Whether the c_0 difference between PE and PPE is sufficient to explain its H_{II} phase is still an open question.

Recent literature has stipulated an interplay between plasmalogens and maintenance of mitochondrial function. Deletion of *PEX26*, reduces cellular levels of ether PLs, including mitochondrial PPE and alkyl ether PC (PC-O), and mitochondrial volume (236). Interestingly, an increase to CL levels was observed, which may compensate for the curvature lost by the reduction in mitochondrial PPE. Notably, these changes occurred independently of alterations to mitochondrial PC and PE levels. Supplementation of plasmalogen precursors reinstated mitochondrial plasmalogen levels and also rescued mitochondrial morphology, suggesting an important interaction between plasmalogens and mitochondrial structure. In the context of disease, recent studies have shown significant alterations to plasmalogen levels in BTHS (247, 248). A *Tafazzin* knockdown mouse model exhibited a major reduction in plasmenyl PC in the heart and PPE in the brain (247, 248), while BTHS patient lymphoblasts exhibited reductions in PPE (248). The depletion of brain PPE levels occurs despite no change to CL levels, suggesting a potential for non-CL effects in BTHS. More recently, Bozelli *et al.* tested whether administration of ether lipid precursors would ameliorate mitochondrial lipid defects in BTHS lymphoblasts. Interestingly, the authors observed a restoration of mitochondrial potential, and an increase in CL levels, implying that regulation of plasmalogen and CL levels may be interlinked (249).

Among non-PL membrane components, sterols are the most abundant in mitochondrial membranes. The predominant sterol in humans is cholesterol, while fungi and plants contain structurally similar molecules, ergosterol, and phytosterols. Despite sterol synthesis originating in the ER, cholesterol is primarily transported to later secretory compartments and the plasma membrane (250). However, sterol levels are still considerable in mitochondria, albeit lower than at the plasma membrane or Golgi; they are also more abundant in the mitochondria of organisms such as plants and yeast than in mammalian cells (9, 250). Mitochondria are the sites of crucial sterol-requiring processes, such as steroid and oxysterol synthesis (21, 251). It is an open question to what extent sterols support the structure and dynamics of mitochondrial membranes, given that they impact nearly all aspects of membrane biophysical properties. Indeed, cholesterol accumulation within mitochondria has been shown to induce mitochondrial dysfunction predominantly through disruption of the respiratory chain and ROS homeostasis (252–255). In addition, reduced ATP synthesis is observed in conditions of increased mitochondrial sterol content, but is ameliorated when normal levels are restored, suggesting a link between sterol abundance and respiratory metabolism (256). In yeast, ergosterol levels have also been correlated with the maintenance of mtDNA (257).

Paradoxically, sterols stiffen membranes (258, 259), but can also act to stabilize highly curved membrane structures in a range of systems. Sterols themselves have a large, negative c_0 owing to their small head groups, but their biophysical properties are based on their interactions with neighboring lipids, as they strongly influence the confirmations and phase properties of acyl chains. Many studies have demonstrated the role of cholesterol and other sterols in rigidifying membranes and promoting ordered phases (259, 260). However, cholesterol also contributes to the adoption of the H_{II} phase in DOPC monolayers (261), and the destabilization of PE H_{II} phases (262, 263), suggesting potential roles in modulating lipid topologies that resemble nonlamellar phases, which are particularly relevant for membrane fission/fusion. It has also been proposed that the negative spontaneous curvature of sterols can contribute to dynamic softening due to their sorting into regions of high curvature (63). Such a redistribution could be especially relevant for stabilizing fusion or fission pores (264). A classical biological example of the role of cholesterol in high-curvature membranes is in clathrin-mediated endocytosis. It has long been observed that cholesterol depletion disrupts clathrin-mediated endocytosis, but more recent evidence has suggested that cholesterol is specifically required for membrane curvature generation at the endocytic pit neck, thereby regulating scission events for proper vesicle fission (265). Based on this evidence, it is plausible that cholesterol could play a similar role in curvature generation for mitochondrial fission, or maintaining lipid curvature in CMs. Interestingly, cholesterol accumulation in mouse liver mitochondria results in altered cristae shapes (254), and cholesterol

increases dynamin-related protein 1 activity at intermediate levels of CL in vitro, suggesting a potential in dynamin-related protein 1–mediated mitochondrial fission (266).

CONCLUSIONS AND OUTLOOK

While it has been over 30 years since the metabolism and biophysical properties of many mitochondrial lipids were first characterized, we are only now beginning to understand the functional implications of these analyses in shaping mitochondrial structure and function. Here, we review some of the biophysical properties of mitochondrial PLs and propose that their spontaneous curvatures are one parameter in which their metabolism and regulation can be understood. We propose that further application of biophysical techniques and modeling approaches could help bridge the gap between our understanding of lipid metabolism and physiology in the mitochondrion. Application of techniques like SAXS to directly measure the properties of lipids from biological samples (45) could be further applied to biochemically isolated mitochondria in conjunction with classic lipidomic approaches. Such analyses can be especially valuable in disease models associated with mitochondrial dysfunction. In addition, the advent of high-resolution electron microscopy analyses of membrane topology in mitochondria has enabled quantitative analysis of membrane curvatures and other geometric parameters (19, 22, 23, 267). These data can be used as the basis for models of mitochondrial metabolism and ATP generation (268) that can connect mitochondrial topological and functional changes with associated changes in lipidome properties in disease states. In this review, we have summarized a variety of literature that has observed aberrant mitochondrial topologies in lipid-driven disorders, implying interplay between lipid composition and morphology/function in mitochondria. We posit that the aforementioned advances in biophysical measurements of lipidome properties will propel an understanding of the regulatory mechanisms governing these pathologies.

Acknowledgments

The authors would like to thank Daniel Milshteyn, Jacob Winnikoff, and Hua Bai for helpful discussions. Marc Morizono provided assistance with figures.

Author contributions

K. V., C. T. L., and I. B. writing–review and editing; K. V., C. T. L., and I. B. writing–original draft; K. V., C. T. L., and I. B. visualization; K. V. and I. B. conceptualization; I. B. resources; I. B. project administration; I. B. funding acquisition.

Author ORCIDs

Kailash Venkatraman https://orcid.org/0000-0001-5138-7610
Christopher T. Lee https://orcid.org/0000-0002-0670-2308
Itay Budin https://orcid.org/0000-0001-9706-4294

Funding and additional information

The National Institutes of Health (NIH) (R35-GM142960 to I. B.) and Department of Energy (DE-SC0022954 to I. B.). Povided financial support. K. V. was supported by the NIH Molecular Biophysics Training Grant (T32-GM008326C). The content is solely the responsibility of the authors and does not necessarily represent the official views of the National Institutes of Health.

Conflict of interest

The authors declare that they have no conflicts of interest with the contents of this article.

Abbreviations

BTHS, Barth syndrome; CDP, cytidine diphosphate; CL, cardiolipin; CM, cristae membrane; DHAP, dihydroxyacetone phosphate; DOPE, dioleoyl phosphatidylethanolamine; ER, endoplasmic reticulum; ETC, electron transport chain; IMM, inner mitochondrial membrane; MD, molecular dynamics; MLCL, monolysocardiolipin; OMM, outer mitochondrial membrane; PA, phosphatidic acid; PC, phosphatidylcholine; PE, phosphatidylethanolamine; PG, phosphatidylglycerol; PI, phosphatidylinositol; PL, phospholipid; PLA_2, phospholipase A_2; PPE, plasmenyl PE; PS, phosphatidylserine; Psd1, phosphatidylserine decarboxylase 1; ROS, reactive oxygen species; SAXS, small angle X-ray scattering; SFA, saturated fatty acid.

Manuscript received August 26, 2024, and in revised form September 13, 2024. Published, JLR Papers in Press, September 18, 2024, https://doi.org/10.1016/j.jlr.2024.100643

REFERENCES

1. Helle, S. C. J., Kanfer, G., Kolar, K., Lang, A., Michel, A. H., and Kornmann, B. (2013) Organization and function of membrane contact sites. *Biochim. Biophys. Acta.* **1833**, 2526–2541
2. Camara, A. K. S., Zhou, Y., Wen, P-C., Tajkhorshid, E., and Kwok, W-M. (2017) Mitochondrial VDACl: a key gatekeeper as potential therapeutic target. *Front. Physiol.* **8**, 460
3. Gupta, A., and Becker, T. (2021) Mechanisms and pathways of mitochondrial outer membrane protein biogenesis. *Biochim. Biophys. Acta Bioenerg.* **1862**, 148323
4. Friedman, J. R., and Nunnari, J. (2014) Mitochondrial form and function. *Nature.* **505**, 335–343
5. Xian, H., and Liou, Y-C. (2021) Functions of outer mitochondrial membrane proteins: mediating the crosstalk between mitochondrial dynamics and mitophagy. *Cell Death Differ.* **28**, 827–842
6. Comte, J., Maïsterrena, B., and Gautheron, D. C. (1976) Lipid composition and protein profiles of outer and inner membranes from pig heart mitochondria. Comparison with microsomes. *Biochim. Biophys. Acta.* **419**, 271–284
7. Daum, G. (1985) Lipids of mitochondria. *Biochim. Biophys. Acta.* **822**, 1–42
8. Zinser, E., Sperka-Gottlieb, C. D., Fasch, E. V., Kohlwein, S. D., Paltauf, F., and Daum, G. (1991) Phospholipid synthesis and lipid composition of subcellular membranes in the unicellular eukaryote Saccharomyces cerevisiae. *J. Bacteriol.* **173**, 2026–2034
9. Horvath, S. E., and Daum, G. (2013) Lipids of mitochondria. *Prog. Lipid Res.* **52**, 590–614

10. Lu, Y-W., and Claypool, S. M. (2015) Disorders of phospholipid metabolism: an emerging class of mitochondrial disease due to defects in nuclear genes. *Front. Genet.* **6**, 3
11. Raja, V., Reynolds, C. A., and Greenberg, M. L. (2017) Barth syndrome: a life-threatening disorder caused by abnormal cardiolipin remodeling. *J. Rare Dis. Res. Treat.* **2**, 58–62
12. Keller, M. A. (2021) Interpreting phospholipid and cardiolipin profiles in rare mitochondrial diseases. *Curr. Opin. Syst. Biol.* **28**, 100383
13. Joshi, A., Richard, T. H., and Gohil, V. M. (2023) Mitochondrial phospholipid metabolism in health and disease. *J. Cell Sci.* **136**, jcs260857
14. Barbot, M., Jans, D. C., Schulz, C., Denkert, N., Kroppen, B., Hoppert, M., *et al.* (2015) Mic10 oligomerizes to bend mitochondrial inner membranes at cristae junctions. *Cell Metab.* **21**, 756–763
15. Basu Ball, W., Neff, J. K., and Gohil, V. M. (2018) The role of nonbilayer phospholipids in mitochondrial structure and function. *FEBS Lett.* **592**, 1273–1290
16. Blum, T. B., Hahn, A., Meier, T., Davies, K. M., and Kühlbrandt, W. (2019) Dimers of mitochondrial ATP synthase induce membrane curvature and self-assemble into rows. *Proc. Natl. Acad. Sci. U. S. A.* **116**, 4250–4255
17. Yang, Z., Wang, L., Yang, C., Pu, S., Guo, Z., Wu, Q., *et al.* (2021) Mitochondrial membrane remodeling. *Front. Bioeng. Biotechnol.* **9**, 786806
18. Mühleip, A., Flygaard, R. K., Baradaran, R., Haapanen, O., Gruhl, T., Tobiasson, V., *et al.* (2023) Structural basis of mitochondrial membrane bending by the I–II–III2–IV2 supercomplex. *Nature.* **615**, 934–938
19. Venkatraman, K., Lee, C. T., Garcia, G. C., Mahapatra, A., Milshteyn, D., Perkins, G., *et al.* (2023) Cristae formation is a mechanical buckling event controlled by the inner mitochondrial membrane lipidome. *EMBO J.* **42**, e114054
20. Bozelli, J. C., Jr., and Epand, R. M. (2022) Interplay between cardiolipin and plasmalogens in Barth syndrome. *J. Inherit. Metab. Dis.* **45**, 99–110
21. Goicoechea, L., Conde de la Rosa, L., Torres, S., García-Ruiz, C., and Fernández-Checa, J. C. (2023) Mitochondrial cholesterol: metabolism and impact on redox biology and disease. *Redox Biol.* **61**, 102643
22. Lee, C. T., Laughlin, J. G., Angliviel de La Beaumelle, N., Amaro, R. E., McCammon, J. A., Ramamoorthi, R., *et al.* (2020) 3D mesh processing using GAMer 2 to enable reaction-diffusion simulations in realistic cellular geometries. *PLoS Comput. Biol.* **16**, e1007756
23. Mendelsohn, R., Garcia, G. C., Bartol, T. M., Lee, C. T., Khandelwal, P., Liu, E., *et al.* (2022) Morphological principles of neuronal mitochondria. *J. Comp. Neurol.* **530**, 886–902
24. Bensley, R. R., and Hoerr, N. L. (1934) Studies on cell structure by the freezing-drying method VI. The preparation and properties of mitochondria. *Anat. Rec.* **60**, 449–455
25. Claude, A. (1946) Fractionation of mammalian liver cells by differential centrifugation: Ii. Experimental procedures and results. *J. Exp. Med.* **84**, 61–89
26. Hogeboom, G. H., Schneider, W. C., and Pallade, G. E. (1948) Cytochemical studies of mammalian tissues; isolation of intact mitochondria from rat liver; some biochemical properties of mitochondria and submicroscopic particulate material. *J. Biol. Chem.* **172**, 619–635
27. Kennedy, E. P., and Lehninger, A. L. (1949) Oxidation of fatty acids and tricarboxylic acid cycle intermediates by isolated rat liver mitochondria. *J. Biol. Chem.* **179**, 957–972
28. Liao, P-C., Bergamini, C., Fato, R., Pon, L. A., and Pallotti, F. (2020) Isolation of mitochondria from cells and tissues. *Methods Cell Biol.* **155**, 3–31
29. Han, X., Yang, K., Yang, J., Cheng, H., and Gross, R. W. (2006) Shotgun lipidomics of cardiolipin molecular species in lipid extracts of biological samples. *J. Lipid Res.* **47**, 864–879
30. Kiebish, M. A., Han, X., and Seyfried, T. N. (2009) Examination of the brain mitochondrial lipidome using shotgun lipidomics. *Methods Mol. Biol.* **579**, 3–18
31. Bird, S. S., Marur, V. R., Stavrovskaya, I. G., and Kristal, B. S. (2013) Qualitative characterization of the rat liver mitochondrial lipidome using LC-MS profiling and high energy collisional dissociation (HCD) all ion fragmentation. *Metabolomics.* **9**, 67–83
32. Baile, M. G., Sathappa, M., Lu, Y-W., Pryce, E., Whited, K., Michael McCaffery, J., *et al.* (2014) Unremodeled and remodeled cardiolipin are functionally indistinguishable in yeast. *J. Biol. Chem.* **289**, 1768–1778
33. Pollard, A. K., Ortori, C. A., Stöger, R., Barrett, D. A., and Chakrabarti, L. (2017) Mouse mitochondrial lipid composition is defined by age in brain and muscle. *Aging.* **9**, 986–998
34. Sileikyte, J., Petronilli, V., Zulian, A., Dabbeni-Sala, F., Tognon, G., Nikolov, P., *et al.* (2011) Regulation of the inner membrane mitochondrial permeability transition by the outer membrane translocator protein (peripheral benzodiazepine receptor). *J. Biol. Chem.* **286**, 1046–1053
35. Nishimura, N., and Yano, M. (2014) Separation of the inner and outer mitochondrial membrane in HeLa cells. *Bio Protoc.* **4**, e1299
36. Rodríguez Graciani, K. M., Chapa-Dubocq, X. R., and Javadov, S. (2019) Challenges in the separation of purified cardiac mitochondrial membranes. *FASEB J.* **33**. https://doi.org/10.1096/fasebj.2019.33.1_supplement.526.2
37. Noterman, M. F., Chaubey, K., Lin-Rahardja, K., Rajadhyaksha, A. M., Pieper, A. A., and Taylor, E. B. (2021) Dual-process brain mitochondria isolation preserves function and clarifies protein composition. *Proc. Natl. Acad. Sci. U. S. A.* **118**, e2019046118
38. Marsh, D. (1996) Intrinsic curvature in normal and inverted lipid structures and in membranes. *Biophys. J.* **70**, 2248–2255
39. Caselli, L., Conti, L., De Santis, I., and Berti, D. (2024) Small-angle X-ray and neutron scattering applied to lipid-based nanoparticles: recent advancements across different length scales. *Adv. Colloid Interf. Sci.* **327**, 103156
40. Kollmitzer, B., Heftberger, P., Rappolt, M., and Pabst, G. (2013) Monolayer spontaneous curvature of raft-forming membrane lipids. *Soft Matter.* **9**, 10877–10884
41. Frewein, M. P. K., Rumetshofer, M., and Pabst, G. (2019) Global small-angle scattering data analysis of inverted hexagonal phases. *J. Appl. Crystallogr.* **52**, 403–414
42. Ramezanpour, M., Schmidt, M. L., Bashe, B. Y. M., Pruim, J. R., Link, M. L., Cullis, P. R., *et al.* (2020) Structural properties of inverted hexagonal phase: a hybrid computational and experimental approach. *Langmuir.* **36**, 6668–6680
43. Fuller, N., and Rand, R. P. (2001) The influence of lysolipids on the spontaneous curvature and bending elasticity of phospholipid membranes. *Biophys. J.* **81**, 243–254
44. Dymond, M. K. (2021) Lipid monolayer spontaneous curvatures: a collection of published values. *Chem. Phys. Lipids.* **239**, 105117
45. Winnikoff, J. R., Milshteyn, D., Vargas-Urbano, S. J., Pedraza-Joya, M. A., Armando, A. M., Quehenberger, O., *et al.* (2024) Homeocurvature adaptation of phospholipids to pressure in deep-sea invertebrates. *Science.* **384**, 1482–1488
46. Tate, M. W., and Gruner, S. M. (1989) Temperature dependence of the structural dimensions of the inverted hexagonal (HII) phase of phosphatidylethanolamine-containing membranes. *Biochemistry.* **28**, 4245–4253
47. Rand, R. P., Fuller, N. L., Gruner, S. M., and Parsegian, V. A. (1990) Membrane curvature, lipid segregation, and structural transitions for phospholipids under dual-solvent stress. *Biochemistry.* **29**, 76–87
48. Fuller, N., Benatti, C. R., and Rand, R. P. (2003) Curvature and bending constants for phosphatidylserine-containing membranes. *Biophys. J.* **85**, 1667–1674
49. Kooijman, E. E., Chupin, V., Fuller, N. L., Kozlov, M. M., de Kruijff, B., Burger, K. N. J., *et al.* (2005) Spontaneous curvature of phosphatidic acid and lysophosphatidic acid. *Biochemistry.* **44**, 2097–2102
50. Chen, Y-F., Tsang, K-Y., Chang, W-F., and Fan, Z-A. (2015) Differential dependencies on [Ca^2] and temperature of the monolayer spontaneous curvatures of DOPE, DOPA and cardiolipin: effects of modulating the strength of the interheadgroup repulsion. *Soft Matter.* **11**, 4041–4053
51. Semeraro, E. F., Marx, L., Frewein, M. P. K., and Pabst, G. (2021) Increasing complexity in small-angle X-ray and neutron scattering experiments: from biological membrane mimics to live cells. *Soft Matter.* **17**, 222–232
52. Mulet, X., Templer, R. H., Woscholski, R., and Ces, O. (2008) Evidence that phosphatidylinositol promotes curved membrane interfaces. *Langmuir.* **24**, 8443–8447
53. Cullis, P. R., Verkleij, A. J., and Ververgaert, P. H. (1978) Polymorphic phase behaviour of cardiolipin as detected by 31P

NMR and freeze-fracture techniques. Effects of calcium, dibucaine and chlorpromazine. *Biochim. Biophys. Acta.* **513**, 11–20
54. Morein, S., Andersson, A., Rilfors, L., and Lindblom, G. (1996) Wild-type Escherichia coli cells regulate the membrane lipid composition in a "window" between gel and non-lamellar structures. *J. Biol. Chem.* **271**, 6801–6809
55. Sinensky, M. (1974) Homeoviscous adaptation—a homeostatic process that regulates the viscosity of membrane lipids in Escherichia coli. *Proc. Natl. Acad. Sci. U. S. A.* **71**, 522–525
56. Hovius, R., Lambrechts, H., Nicolay, K., and de Kruijff, B. (1990) Improved methods to isolate and subfractionate rat liver mitochondria. Lipid composition of the inner and outer membrane. *Biochim. Biophys. Acta Biomembr.* **1021**, 217–226
57. McMahon, H. T., and Gallop, J. L. (2005) Membrane curvature and mechanisms of dynamic cell membrane remodelling. *Nature.* **438**, 590–596
58. Chabanon, M., Stachowiak, J. C., and Rangamani, P. (2017) Systems biology of cellular membranes: a convergence with biophysics. *Wiley Interdiscip. Rev. Syst. Biol. Med.* **9**. https://doi.org/10.1002/wsbm.1386
59. Harb, J. S., Comte, J., and Gautheron, D. C. (1981) Asymmetrical orientation of phospholipids and their interactions with marker enzymes in pig heart mitochondrial inner membrane. *Arch. Biochem. Biophys.* **208**, 305–318
60. Gallet, P. F., Petit, J. M., Maftah, A., Zachowski, A., and Julien, R. (1997) Asymmetrical distribution of cardiolipin in yeast inner mitochondrial membrane triggered by carbon catabolite repression. *Biochem. J.* **324**, 627–634
61. Kagan, V. E., Chu, C. T., Tyurina, Y. Y., Cheikhi, A., and Bayir, H. (2014) Cardiolipin asymmetry, oxidation and signaling. *Chem. Phys. Lipids.* **179**, 64–69
62. Hossein, A., and Deserno, M. (2020) Spontaneous curvature, differential stress, and bending modulus of asymmetric lipid membranes. *Biophys. J.* **118**, 624–642
63. Lessen, H. J., Sapp, K. C., Beaven, A. H., Ashkar, R., and Sodt, A. J. (2022) Molecular mechanisms of spontaneous curvature and softening in complex lipid bilayer mixtures. *Biophys. J.* **121**, 3188–3199
64. McMahon, H. T., and Boucrot, E. (2015) Membrane curvature at a glance. *J. Cell Sci.* **128**, 1065–1070
65. Beltrán-Heredia, E., Tsai, F-C., Salinas-Almaguer, S., Cao, F. J., Bassereau, P., and Monroy, F. (2019) Membrane curvature induces cardiolipin sorting. *Commun. Biol.* **2**. https://doi.org/10.1038/s42003-019-0471-x
66. [preprint] Doktorova, M., Symons, J. L., Zhang, X., Wang, H-Y., Schlegel, J., Lorent, J. H., *et al.* (2023) Cell membranes sustain phospholipid imbalance via cholesterol asymmetry. *bioRxiv.* https://doi.org/10.1101/2023.07.30.551157v1
67. Pabst, G., and Keller, S. (2024) Exploring membrane asymmetry and its effects on membrane proteins. *Trends Biochem. Sci.* **49**, 333–345
68. Fanani, M. L., and Ambroggio, E. E. (2023) Phospholipases and membrane curvature: what is happening at the surface? *Membranes.* **13**, 190
69. Takada, N., Naito, T., Inoue, T., Nakayama, K., Takatsu, H., and Shin, H. (2018) Phospholipid-flipping activity of P4-ATPase drives membrane curvature. *EMBO J.* **37**, e97705
70. Liu, J., Epand, R. F., Durrant, D., Grossman, D., Chi, N-W., Epand, R. M., *et al.* (2008) Role of phospholipid scramblase 3 in the regulation of tumor necrosis factor-α-induced apoptosis. *Biochemistry.* **47**, 4518–4529
71. Osman, C., Voelker, D. R., and Langer, T. (2011) Making heads or tails of phospholipids in mitochondria. *J. Cell Biol.* **192**, 7–16
72. Luévano-Martínez, L. A., and Kowaltowski, A. J. (2017) Topological characterization of the mitochondrial phospholipid scramblase 3. *FEBS Lett.* **591**, 4056–4066
73. Jahn, H., Bartoš, L., Dearden, G. I., Dittman, J. S., Holthuis, J. C. M., Vácha, R., *et al.* (2023) Phospholipids are imported into mitochondria by VDAC, a dimeric beta barrel scramblase. *Nat. Commun.* **14**, 8115
74. Epand, R. F., Tokarska-Schlattner, M., Schlattner, U., Wallimann, T., and Epand, R. M. (2007) Cardiolipin clusters and membrane domain formation induced by mitochondrial proteins. *J. Mol. Biol.* **365**, 968–980
75. [preprint] Zuccaro, K. E., Abriata, L. A., Meireles, F. T. P., Moss, F. R., Frost, A., Peraro, M. D., *et al.* (2024) Cardiolipin clustering promotes mitochondrial membrane dynamics. *bioRxiv.* https://doi.org/10.1101/2024.05.21.595226
76. Pfeiffer, K., Gohil, V., Stuart, R. A., Hunte, C., Brandt, U., Greenberg, M. L., *et al.* (2003) Cardiolipin stabilizes respiratory chain supercomplexes. *J. Biol. Chem.* **278**, 52873–52880
77. Mehdipour, A. R., and Hummer, G. (2016) Cardiolipin puts the seal on ATP synthase. *Proc. Natl. Acad. Sci. U. S. A.* **113**, 8568–8570
78. Mühleip, A., McComas, S. E., and Amunts, A. (2019) Structure of a mitochondrial ATP synthase with bound native cardiolipin. *Elife.* **8**, e51179
79. Brown, M. F. (2012) Curvature forces in membrane lipid-protein interactions. *Biochemistry.* **51**, 9782–9795
80. Flis, V. V., and Daum, G. (2013) Lipid transport between the endoplasmic reticulum and mitochondria. *Cold Spring Harb. Perspect. Biol.* **5**, a013235
81. Acoba, M. G., Senoo, N., and Claypool, S. M. (2020) Phospholipid ebb and flow makes mitochondria go. *J. Cell Biol.* **219**, e202003131
82. Kennedy, E. P., and Weiss, S. B. (1956) The function of cytidine coenzymes in the biosynthesis of phospholipides. *J. Biol. Chem.* **222**, 193–214
83. Borkenhagen, L. F., Kennedy, E. P., and Fielding, L. (1961) Enzymatic Formation and decarboxylation of phosphatidylserine. *J. Biol. Chem.* **236**, PC28–PC30
84. Clancey, C. J., Chang, S. C., and Dowhan, W. (1993) Cloning of a gene (PSD1) encoding phosphatidylserine decarboxylase from Saccharomyces cerevisiae by complementation of an Escherichia coli mutant. *J. Biol. Chem.* **268**, 24580–24590
85. Trotter, P. J., Pedretti, J., and Voelker, D. R. (1993) Phosphatidylserine decarboxylase from Saccharomyces cerevisiae. Isolation of mutants, cloning of the gene, and creation of a null allele. *J. Biol. Chem.* **268**, 21416–21424
86. Tamura, Y., Onguka, O., Itoh, K., Endo, T., Iijima, M., Claypool, S. M., *et al.* (2012) Phosphatidylethanolamine biosynthesis in mitochondria: phosphatidylserine (PS) trafficking is independent of a PS decarboxylase and intermembrane space proteins UPS1P and UPS2P. *J. Biol. Chem.* **287**, 43961–43971
87. Potting, C., Wilmes, C., Engmann, T., Osman, C., and Langer, T. (2010) Regulation of mitochondrial phospholipids by Ups1/PRELI-like proteins depends on proteolysis and Mdm35. *EMBO J.* **29**, 2888–2898
88. Connerth, M., Tatsuta, T., Haag, M., Klecker, T., Westermann, B., and Langer, T. (2012) Intramitochondrial transport of phosphatidic acid in yeast by a lipid transfer protein. *Science.* **338**, 815–818
89. Potting, C., Tatsuta, T., König, T., Haag, M., Wai, T., Aaltonen, M. J., *et al.* (2013) TRIAP1/PRELI complexes prevent apoptosis by mediating intramitochondrial transport of phosphatidic acid. *Cell Metab.* **18**, 287–295
90. Watanabe, Y., Tamura, Y., Kawano, S., and Endo, T. (2015) Structural and mechanistic insights into phospholipid transfer by Ups1–Mdm35 in mitochondria. *Nat. Commun.* **6**, 7922
91. Osman, C., Haag, M., Wieland, F. T., Brügger, B., and Langer, T. (2010) A mitochondrial phosphatase required for cardiolipin biosynthesis: the PGP phosphatase Gep4. *EMBO J.* **29**, 1976–1987
92. Tamura, Y., Harada, Y., Nishikawa, S-I., Yamano, K., Kamiya, M., Shiota, T., *et al.* (2013) Tam41 is a CDP-diacylglycerol synthase required for cardiolipin biosynthesis in mitochondria. *Cell Metab.* **17**, 709–718
93. Chang, S-C., Heacock, P. N., Clancey, C. J., and Dowhan, W. (1998) The PEL1 Gene (Renamed PGS1) Encodes the phosphatidylglycero-phosphate synthase ofSaccharomyces cerevisiae. *J. Biol. Chem.* **273**, 9829–9836
94. Joshi, A. S., Zhou, J., Gohil, V. M., Chen, S., and Greenberg, M. L. (2009) Cellular functions of cardiolipin in yeast. *Biochim. Biophys. Acta.* **1793**, 212–218
95. Blunsom, N. J., and Cockcroft, S. (2020) CDP-diacylglycerol synthases (CDS): gateway to phosphatidylinositol and cardiolipin synthesis. *Front. Cell Dev. Biol.* **8**, 63
96. Jiang, F., Rizavi, H. S., and Greenberg, M. L. (1997) Cardiolipin is not essential for the growth of Saccharomyces cerevisiae on fermentable or non-fermentable carbon sources. *Mol. Microbiol.* **26**, 481–491
97. Chang, S. C., Heacock, P. N., Mileykovskaya, E., Voelker, D. R., and Dowhan, W. (1998) Isolation and characterization of the gene (CLS1) encoding cardiolipin synthase in Saccharomyces cerevisiae. *J. Biol. Chem.* **273**, 14933–14941
98. Schlame, M., and Greenberg, M. L. (2017) Biosynthesis, remodeling and turnover of mitochondrial cardiolipin. *Biochim. Biophys. Acta Mol. Cell Biol. Lipids.* **1862**, 3–7

99. Steenbergen, R., Nanowski, T. S., Beigneux, A., Kulinski, A., Young, S. G., and Vance, J. E. (2005) Disruption of the phosphatidylserine decarboxylase gene in mice causes embryonic lethality and mitochondrial defects. *J. Biol. Chem.* **280**, 40032–40040
100. Kasahara, T., Kubota-Sakashita, M., Nagatsuka, Y., Hirabayashi, Y., Hanasaka, T., Tohyama, K., *et al.* (2020) Cardiolipin is essential for early embryonic viability and mitochondrial integrity of neurons in mammals. *FASEB J.* **34**, 1465–1480
101. Tasseva, G., Bai, H. D., Davidescu, M., Haromy, A., Michelakis, E., and Vance, J. E. (2013) Phosphatidylethanolamine deficiency in Mammalian mitochondria impairs oxidative phosphorylation and alters mitochondrial morphology. *J. Biol. Chem.* **288**, 4158–4173
102. Gohil, V. M., Thompson, M. N., and Greenberg, M. L. (2005) Synthetic lethal interaction of the mitochondrial phosphatidylethanolamine and cardiolipin biosynthetic pathways in Saccharomyces cerevisiae. *J. Biol. Chem.* **280**, 35410–35416
103. Mileykovskaya, E., and Dowhan, W. (2014) Cardiolipin-dependent formation of mitochondrial respiratory supercomplexes. *Chem. Phys. Lipids.* **179**, 42–48
104. Baker, C. D., Basu Ball, W., Pryce, E. N., and Gohil, V. M. (2016) Specific requirements of nonbilayer phospholipids in mitochondrial respiratory chain function and formation. *Mol. Biol. Cell.* **27**, 2161–2171
105. Calzada, E., Avery, E., Sam, P. N., Modak, A., Wang, C., McCaffery, J. M., *et al.*Han, X., Alder, N. N., and Claypool, S. M. (2019) Phosphatidylethanolamine made in the inner mitochondrial membrane is essential for yeast cytochrome bcl complex function. *Nat. Commun.* **10**, 1432
106. Tillman, T. S., and Cascio, M. (2003) Effects of membrane lipids on ion channel structure and function. *Cell Biochem. Biophys.* **38**, 161–190
107. Budin, I., de Rond, T., Chen, Y., Chan, L. J. G., Petzold, C. J., and Keasling, J. D. (2018) Viscous control of cellular respiration by membrane lipid composition. *Science.* **362**, 1186–1189
108. Gupte, S., Wu, E-S., Hoechli, L., Hoechli, M., Jacobson, K., Sowers, A. E., *et al.* (1984) Relationship between lateral diffusion, collision frequency, and electron transfer of mitochondrial inner membrane oxidation-reduction components. *Proc. Natl. Acad. Sci. U. S. A.* **81**, 2606–2610
109. Lewis, R. N., Mannock, D. A., McElhaney, R. N., Turner, D. C., and Gruner, S. M. (1989) Effect of fatty acyl chain length and structure on the lamellar gel to liquid-crystalline and lamellar to reversed hexagonal phase transitions of aqueous phosphatidylethanolamine dispersions. *Biochemistry.* **28**, 541–548
110. Szule, J. A., Fuller, N. L., and Rand, R. P. (2002) The effects of acyl chain length and saturation of diacylglycerols and phosphatidylcholines on membrane monolayer curvature. *Biophys. J.* **83**, 977–984
111. Teague, W. E., Jr., Soubias, O., Petrache, H., Fuller, N., Hines, K. G., Rand, R. P., *et al.* (2013) Elastic properties of polyunsaturated phosphatidylethanolamines influence rhodopsin function. *Faraday Discuss.* **161**, 383–395
112. Lewis, R. N. A. H., and McElhaney, R. N. (2009) The physicochemical properties of cardiolipin bilayers and cardiolipin-containing lipid membranes. *Biochim. Biophys. Acta.* **1788**, 2069–2079
113. Renne, M. F., Bao, X., Hokken, M. W. J., Bierhuizen, A. S., Hermansson, M., Sprenger, R. R., *et al.* (2022) Molecular species selectivity of lipid transport creates a mitochondrial sink for diunsaturated phospholipids. *EMBO J.* **41**, e106837
114. Heikinheimo, L., and Somerharju, P. (1998) Preferential decarboxylation of hydrophilic phosphatidylserine species in cultured cells. Implications on the mechanism of transport to mitochondria and cellular aminophospholipid species compositions. *J. Biol. Chem.* **273**, 3327–3335
115. Heikinheimo, L., and Somerharju, P. (2002) Translocation of phosphatidylthreonine and -serine to mitochondria diminishes exponentially with increasing molecular hydrophobicity. *Traffic.* **3**, 367–377
116. Wong, A. M., and Budin, I. (2024) Organelle-targeted Laurdans measure heterogeneity in subcellular membranes and their responses to saturated lipid stress. *ACS Chem. Biol.* **19**, 1773–1785
117. Sparagna, G. C., Hickson-Bick, D. L., Buja, L. M., and McMillin, J. B. (2000) A metabolic role for mitochondria in palmitate-induced cardiac myocyte apoptosis. *Am. J. Physiol. Heart Circ. Physiol.* **279**, H2124–H2132
118. Ostrander, D. B., Sparagna, G. C., Amoscato, A. A., McMillin, J. B., and Dowhan, W. (2001) Decreased cardiolipin synthesis corresponds with cytochrome c release in palmitate-induced cardiomyocyte apoptosis. *J. Biol. Chem.* **276**, 38061–38067
119. Crescenzo, R., Bianco, F., Mazzoli, A., Giacco, A., Cancelliere, R., di Fabio, G., *et al.* (2015) Fat quality influences the obesogenic effect of high fat diets. *Nutrients.* **7**, 9475–9491
120. Ruiz-Ramírez, A., Barrios-Maya, M-A., López-Acosta, O., Molina-Ortiz, D., and El-Hafidi, M. (2015) Cytochrome c release from rat liver mitochondria is compromised by increased saturated cardiolipin species induced by sucrose feeding. *Am. J. Physiol. Endocrinol. Metab.* **309**, E777–E786
121. Sullivan, E. M., Pennington, E. R., Green, W. D., Beck, M. A., Brown, D. A., and Shaikh, S. R. (2018) Mechanisms by which dietary fatty acids regulate mitochondrial structure-function in health and disease. *Adv. Nutr.* **9**, 247–262
122. Begriche, K., Massart, J., Robin, M-A., Bonnet, F., and Fromenty, B. (2013) Mitochondrial adaptations and dysfunctions in nonalcoholic fatty liver disease. *Hepatology.* **58**, 1497–1507
123. Parks, E., Yki-Järvinen, H., and Hawkins, M. (2017) Out of the frying pan: dietary saturated fat influences nonalcoholic fatty liver disease. *J. Clin. Invest.* **127**, 454–456
124. Meex, R. C. R., and Blaak, E. E. (2021) Mitochondrial dysfunction is a key pathway that links saturated fat intake to the development and progression of NAFLD. *Mol. Nutr. Food Res.* **65**, e1900942
125. Li, Z., Agellon, L. B., Allen, T. M., Umeda, M., Jewell, L., Mason, A., *et al.* (2006) The ratio of phosphatidylcholine to phosphatidylethanolamine influences membrane integrity and steatohepatitis. *Cell Metab.* **3**, 321–331
126. van der Veen, J. N., Kennelly, J. P., Wan, S., Vance, J. E., Vance, D. E., and Jacobs, R. L. (2017) The critical role of phosphatidylcholine and phosphatidylethanolamine metabolism in health and disease. *Biochim. Biophys. Acta Biomembr.* **1859**, 1558–1572
127. Grapentine, S., and Bakovic, M. (2019) Significance of bilayer-forming phospholipids for skeletal muscle insulin sensitivity and mitochondrial function. *J. Biomed. Res.* **34**, 1–13
128. van der Veen, J. N., Lingrell, S., da Silva, R. P., Jacobs, R. L., and Vance, D. E. (2014) The concentration of phosphatidylethanolamine in mitochondria can modulate ATP production and glucose metabolism in mice. *Diabetes.* **63**, 2620–2630
129. Kim, J-A., Wei, Y., and Sowers, J. R. (2008) Role of mitochondrial dysfunction in insulin resistance. *Circ. Res.* **102**, 401–414
130. Bournat, J. C., and Brown, C. W. (2010) Mitochondrial dysfunction in obesity. *Curr. Opin. Endocrinol. Diabetes Obes.* **17**, 446–452
131. Pinti, M. V., Fink, G. K., Hathaway, Q. A., Durr, A. J., Kunovac, A., and Hollander, J. M. (2019) Mitochondrial dysfunction in type 2 diabetes mellitus: an organ-based analysis. *Am. J. Physiol. Endocrinol. Metab.* **316**, E268–E285
132. Fromenty, B., and Roden, M. (2023) Mitochondrial alterations in fatty liver diseases. *J. Hepatol.* **78**, 415–429
133. Lecocq, J., and Ballou, C. E. (1964) ON the structure of cardiolipin. *Biochemistry.* **3**, 976–980
134. Hübner, W., Mantsch, H. H., and Kates, M. (1991) Intramolecular hydrogen bonding in cardiolipin. *Biochim. Biophys. Acta.* **1066**, 166–174
135. Kates, M., Syz, J. Y., Gosser, D., and Haines, T. H. (1993) pH-dissociation characteristics of cardiolipin and its 2'-deoxy analogue. *Lipids.* **28**, 877–882
136. Haines, T. H., and Dencher, N. A. (2002) Cardiolipin: a proton trap for oxidative phosphorylation. *FEBS Lett.* **528**, 35–39
137. Lewis, R. N. A. H., and McElhaney, R. N. (2000) Surface charge markedly attenuates the nonlamellar phase-forming propensities of lipid bilayer membranes: calorimetric and 31P-nuclear magnetic resonance studies of mixtures of cationic, anionic, and zwitterionic lipids. *Biophys. J.* **79**, 1455–1464
138. Olofsson, G., and Sparr, E. (2013) Ionization constants pKa of cardiolipin. *PLoS One.* **8**, e73040
139. Malyshka, D., Pandiscia, L. A., and Schweitzer-Stenner, R. (2014) Cardiolipin containing liposomes are fully ionized at physiological pH. An FT-IR study of phosphate group ionization. *Vib. Spectrosc.* **75**, 86–92

140. Sathappa, M., and Alder, N. N. (2016) The ionization properties of cardiolipin and its variants in model bilayers. *Biochim. Biophys. Acta Biomembr.* **1858**, 1362–1372
141. Khalifat, N., Puff, N., Bonneau, S., Fournier, J-B., and Angelova, M. I. (2008) Membrane deformation under local pH gradient: mimicking mitochondrial cristae dynamics. *Biophys. J.* **95**, 4924–4933
142. Khalifat, N., Fournier, J-B., Angelova, M. I., and Puff, N. (2011) Lipid packing variations induced by pH in cardiolipin-containing bilayers: the driving force for the cristae-like shape instability. *Biochim. Biophys. Acta Biomembr.* **1808**, 2724–2733
143. Sturm, M., Gutowski, O., and Brezesinski, G. (2022) The effect of pH on the structure and lateral organization of cardiolipin in Langmuir monolayers. *Chemphyschem.* **23**, e202200218
144. Mileykovskaya, E., and Dowhan, W. (2000) Visualization of phospholipid domains in Escherichia coli by using the cardiolipin-specific fluorescent dye 10-N-nonyl acridine orange. *J. Bacteriol.* **182**, 1172–1175
145. Kawai, F., Shoda, M., Harashima, R., Sadaie, Y., Hara, H., and Matsumoto, K. (2004) Cardiolipin domains in Bacillus subtilis marburg membranes. *J. Bacteriol.* **186**, 1475–1483
146. Renner, L. D., and Weibel, D. B. (2011) Cardiolipin microdomains localize to negatively curved regions of Escherichia coli membranes. *Proc. Natl. Acad. Sci. U. S. A.* **108**, 6264–6269
147. Rand, R. P., and Sengupta, S. (1972) Cardiolipin forms hexagonal structures with divalent cations. *Biochim. Biophys. Acta.* **255**, 484–492
148. Miranda, É. G. A., Araujo-Chaves, J. C., Kawai, C., Brito, A. M. M., Dias, I. W. R., Arantes, J. T., *et al.* (2019) Cardiolipin structure and oxidation are affected by Ca2+ at the interface of lipid bilayers. *Front. Chem.* **7**, 930
149. Fox, C. A., Ellison, P., Ikon, N., and Ryan, R. O. (2019) Calcium-induced transformation of cardiolipin nanodisks. *Biochim. Biophys. Acta Biomembr.* **1861**, 1030–1036
150. Konar, S., Arif, H., and Allolio, C. (2023) Mitochondrial membrane model: lipids, elastic properties, and the changing curvature of cardiolipin. *Biophys. J.* **122**, 4274–4287
151. Bernardi, P. (1999) Mitochondrial transport of cations: channels, exchangers, and permeability transition. *Physiol. Rev.* **79**, 1127–1155
152. Calvo-Rodriguez, M., Hou, S. S., Snyder, A. C., Kharitonova, E. K., Russ, A. N., Das, S., *et al.* (2020) Increased mitochondrial calcium levels associated with neuronal death in a mouse model of Alzheimer's disease. *Nat. Commun.* **11**, 2146
153. Jung, H., Kim, S. Y., Canbakis Cecen, F. S., Cho, Y., and Kwon, S-K. (2020) Dysfunction of mitochondrial Ca2+ regulatory machineries in brain aging and neurodegenerative diseases. *Front. Cell Dev. Biol.* **8**, 599792
154. D'Angelo, D., and Rizzuto, R. (2023) The mitochondrial calcium uniporter (MCU): molecular identity and role in human diseases. *Biomolecules.* **13**, 1304
155. Boyd, K. J., Alder, N. N., and May, E. R. (2017) Buckling under pressure: curvature-based lipid segregation and stability modulation in cardiolipin-containing bilayers. *Langmuir.* **33**, 6937–6946
156. Petit, J. M., Huet, O., Gallet, P. F., Maftah, A., Ratinaud, M. H., and Julien, R. (1994) Direct analysis and significance of cardiolipin transverse distribution in mitochondrial inner membranes. *Eur. J. Biochem.* **220**, 871–879
157. Krebs, J. J., Hauser, H., and Carafoli, E. (1979) Asymmetric distribution of phospholipids in the inner membrane of beef heart mitochondria. *J. Biol. Chem.* **254**, 5308–5316
158. Gohil, V. M., Gvozdenovic-Jeremic, J., Schlame, M., and Greenberg, M. L. (2005) Binding of 10-N-nonyl acridine orange to cardiolipin-deficient yeast cells: implications for assay of cardiolipin. *Anal. Biochem.* **343**, 350–352
159. Schlame, M., and Haldar, D. (1993) Cardiolipin is synthesized on the matrix side of the inner membrane in rat liver mitochondria. *J. Biol. Chem.* **268**, 74–79
160. Claypool, S. M., McCaffery, J. M., and Koehler, C. M. (2006) Mitochondrial mislocalization and altered assembly of a cluster of Barth syndrome mutant tafazzins. *J. Cell Biol.* **174**, 379–390
161. Lu, Y-W., Galbraith, L., Herndon, J. D., Lu, Y-L., Pras-Raves, M., Vervaart, M., *et al.* (2016) Defining functional classes of Barth syndrome mutation in humans. *Hum. Mol. Genet.* **25**, 1754–1770
162. Schlame, M., and Xu, Y. (2020) The function of tafazzin, a mitochondrial phospholipid-lysophospholipid acyltransferase. *J. Mol. Biol.* **432**, 5043–5051
163. Liang, Z., Schmidtke, M. W., and Greenberg, M. L. (2022) Current knowledge on the role of cardiolipin remodeling in the context of lipid oxidation and Barth syndrome. *Front. Mol. Biosci.* **9**, 915301
164. Schlame, M. (2013) Cardiolipin remodeling and the function of tafazzin. *Biochim. Biophys. Acta.* **1831**, 582–588
165. Beranek, A., Rechberger, G., Knauer, H., Wolinski, H., Kohlwein, S. D., and Leber, R. (2009) Identification of a cardiolipin-specific phospholipase encoded by the gene CLD1 (YGR110W) in yeast. *J. Biol. Chem.* **284**, 11572–11578
166. Schlame, M., Acehan, D., Berno, B., Xu, Y., Valvo, S., Ren, M., *et al.* (2012) The physical state of lipid substrates provides transacylation specificity for tafazzin. *Nat. Chem. Biol.* **8**, 862–869
167. Abe, M., Hasegawa, Y., Oku, M., Sawada, Y., Tanaka, E., Sakai, Y., *et al.* (2016) Mechanism for remodeling of the acyl chain composition of cardiolipin catalyzed by Saccharomyces cerevisiae tafazzin. *J. Biol. Chem.* **291**, 15491–15502
168. Schlame, M., Xu, Y., and Ren, M. (2017) The basis for acyl specificity in the tafazzin reaction. *J. Biol. Chem.* **292**, 5499–5506
169. Oemer, G., Koch, J., Wohlfarter, Y., Alam, M. T., Lackner, K., Sailer, S., *et al.* (2020) Phospholipid acyl chain diversity controls the tissue-specific assembly of mitochondrial cardiolipins. *Cell Rep.* **30**, 4281–4291.e4
170. Kiebish, M. A., Han, X., Cheng, H., Lunceford, A., Clarke, C. F., Moon, H., *et al.* (2008) Lipidomic analysis and electron transport chain activities in C57BL/6J mouse brain mitochondria. *J. Neurochem.* **106**, 299–312
171. Schlame, M., Ren, M., Xu, Y., Greenberg, M. L., and Haller, I. (2005) Molecular symmetry in mitochondrial cardiolipins. *Chem. Phys. Lipids.* **138**, 38–49
172. Zhou, Y., Peisker, H., and Dörmann, P. (2016) Molecular species composition of plant cardiolipin determined by liquid chromatography mass spectrometry. *J. Lipid Res.* **57**, 1308–1321
173. Chicco, A. J., and Sparagna, G. C. (2007) Role of cardiolipin alterations in mitochondrial dysfunction and disease. *Am. J. Physiol. Cell Physiol.* **292**, C33–C44
174. Claypool, S. M., and Koehler, C. M. (2012) The complexity of cardiolipin in health and disease. *Trends Biochem. Sci.* **37**, 32–41
175. Pennington, E. R., Funai, K., Brown, D. A., and Shaikh, S. R. (2019) The role of cardiolipin concentration and acyl chain composition on mitochondrial inner membrane molecular organization and function. *Biochim. Biophys. Acta Mol. Cell Biol. Lipids.* **1864**, 1039–1052
176. Barth, P. G., Scholte, H. R., Berden, J. A., Van der Klei-Van Moorsel, J. M., Luyt-Houwen, I. E., Van 't Veer-Korthof, E. T., *et al.* (1983) An X-linked mitochondrial disease affecting cardiac muscle, skeletal muscle and neutrophil leucocytes. *J. Neurol. Sci.* **62**, 327–355
177. Adès, L. C., Gedeon, A. K., Wilson, M. J., Latham, M., Partington, M. W., Mulley, J. C., *et al.* (1993) Barth syndrome: clinical features and confirmation of gene localisation to distal Xq28. *Am. J. Med. Genet.* **45**, 327–334
178. Bione, S., D'Adamo, P., Maestrini, E., Gedeon, A. K., Bolhuis, P. A., and Toniolo, D. (1996) A novel X-linked gene, G4.5. is responsible for Barth syndrome. *Nat. Genet.* **12**, 385–389
179. Xu, Y., Sutachan, J. J., Plesken, H., Kelley, R. I., and Schlame, M. (2005) Erratum: characterization of lymphoblast mitochondria from patients with Barth syndrome. *Lab. Invest.* **85**, 831
180. Acehan, D., Xu, Y., Stokes, D. L., and Schlame, M. (2007) Comparison of lymphoblast mitochondria from normal subjects and patients with Barth syndrome using electron microscopic tomography. *Lab. Invest.* **87**, 40–48
181. Vreken, P., Valianpour, F., Nijtmans, L. G., Grivell, L. A., Plecko, B., Wanders, R. J., *et al.* (2000) Defective remodeling of cardiolipin and phosphatidylglycerol in Barth syndrome. *Biochem. Biophys. Res. Commun.* **279**, 378–382
182. Schlame, M., Towbin, J. A., Heerdt, P. M., Jehle, R., DiMauro, S., and Blanck, T. J. J. (2002) Deficiency of tetralinoleoyl-cardiolipin in Barth syndrome. *Ann. Neurol.* **51**, 634–637
183. van Werkhoven, M. A., Thorburn, D. R., Gedeon, A. K., and Pitt, J. J. (2006) Monolysocardiolipin in cultured fibroblasts is a sensitive and specific marker for Barth Syndrome. *J. Lipid Res.* **47**, 2346–2351

184. Byeon, S. K., Ramarajan, M. G., Madugundu, A. K., Oglesbee, D., Vernon, H. J., and Pandey, A. (2021) High-resolution mass spectrometric analysis of cardiolipin profiles in Barth syndrome. *Mitochondrion.* **60**, 27–32
185. Malhotra, A., Edelman-Novemsky, I., Xu, Y., Plesken, H., Ma, J., Schlame, M., *et al.* (2009) Role of calcium-independent phospholipase A2 in the pathogenesis of Barth syndrome. *Proc. Natl. Acad. Sci. U. S. A.* **106**, 2337–2341
186. Wang, G., McCain, M. L., Yang, L., He, A., Pasqualini, F. S., Agarwal, A., *et al.* (2014) Modeling the mitochondrial cardiomyopathy of Barth syndrome with induced pluripotent stem cell and heart-on-chip technologies. *Nat. Med.* **20**, 616–623
187. Zhu, S., 'e Chen, Z., Zhu, M., Shen, Y., Leon, L. J., Chi, L., *et al.* (2021) Cardiolipin remodeling defects impair mitochondrial architecture and function in a murine model of Barth syndrome cardiomyopathy. *Circ. Heart Fail.* **14**, e008289
188. Pu, W. T. (2022) Experimental models of Barth syndrome. *J. Inherit. Metab. Dis.* **45**, 72–81
189. Valianpour, F., Mitsakos, V., Schlemmer, D., Towbin, J. A., Taylor, J. M., Ekert, P. G., *et al.* (2005) Monolysocardiolipins accumulate in Barth syndrome but do not lead to enhanced apoptosis. *J. Lipid Res.* **46**, 1182–1195
190. Saric, A., Andreau, K., Armand, A-S., Møller, I. M., and Petit, P. X. (2015) Barth syndrome: from mitochondrial dysfunctions associated with aberrant production of reactive oxygen species to pluripotent stem cell studies. *Front. Genet.* **6**, 359
191. Anzmann, A. F., Sniezek, O. L., Pado, A., Busa, V., Vaz, F. M., Kreimer, S. D., *et al.* (2021) Diverse mitochondrial abnormalities in a new cellular model of TAFFAZZIN deficiency are remediated by cardiolipin-interacting small molecules. *J. Biol. Chem.* **297**, 101005
192. Venkatraman, K., and Budin, I. (2024) Cardiolipin remodeling maintains the inner mitochondrial membrane in cells with saturated lipidomes. *J. Lipid Res.* **65**, 100601
193. Powell, G. L., and Marsh, D. (1985) Polymorphic phase behavior of cardiolipin derivatives studied by phosphorus-31 NMR and x-ray diffraction. *Biochemistry.* **24**, 2902–2908
194. Duncan, A. L. (2020) Monolysocardiolipin (MLCL) interactions with mitochondrial membrane proteins. *Biochem. Soc. Trans.* **48**, 993–1004
195. Boyd, K. J., Alder, N. N., and May, E. R. (2018) Molecular dynamics analysis of cardiolipin and monolysocardiolipin on bilayer properties. *Biophys. J.* **114**, 2116–2127
196. Lewis, R. N. A. H., Zweytick, D., Pabst, G., Lohner, K., and McElhaney, R. N. (2007) Calorimetric, x-ray diffraction, and spectroscopic studies of the thermotropic phase behavior and organization of tetramyristoyl cardiolipin membranes. *Biophys. J.* **92**, 3166–3177
197. Panov, A. V., and Dikalov, S. I. (2020) Cardiolipin, perhydroxyl radicals, and lipid peroxidation in mitochondrial dysfunctions and aging. *Oxid. Med. Cell Longev.* **2020**, 1323028
198. Falabella, M., Vernon, H. J., Hanna, M. G., Claypool, S. M., and Pitceathly, R. D. S. (2021) Cardiolipin, mitochondria, and neurological disease. *Trends Endocrinol. Metab.* **32**, 224–237
199. Ruggiero, F. M., Cafagna, F., Petruzzella, V., Gadaleta, M. N., and Quagliariello, E. (1992) Lipid composition in synaptic and nonsynaptic mitochondria from rat brains and effect of aging. *J. Neurochem.* **59**, 487–491
200. Sen, T., Sen, N., Jana, S., Khan, F. H., Chatterjee, U., and Chakrabarti, S. (2007) Depolarization and cardiolipin depletion in aged rat brain mitochondria: relationship with oxidative stress and electron transport chain activity. *Neurochem. Int.* **50**, 719–725
201. Petrosillo, G., Matera, M., Casanova, G., Ruggiero, F. M., and Paradies, G. (2008) Mitochondrial dysfunction in rat brain with aging Involvement of complex I, reactive oxygen species and cardiolipin. *Neurochem. Int.* **53**, 126–131
202. Lores-Arnaiz, S., Lombardi, P., Karadayian, A. G., Cutrera, R., and Bustamante, J. (2019) Changes in motor function and brain cortex mitochondrial active oxygen species production in aged mice. *Exp. Gerontol.* **118**, 88–98
203. Lewin, M. B., and Timiras, P. S. (1984) Lipid changes with aging in cardiac mitochondrial membranes. *Mech. Ageing Dev.* **24**, 343–351
204. McMillin, J. B., Taffet, G. E., Taegtmeyer, H., Hudson, E. K., and Tate, C. A. (1993) Mitochondrial metabolism and substrate competition in the aging Fischer rat heart. *Cardiovasc. Res.* **27**, 2222–2228
205. Pepe, S., Tsuchiya, N., Lakatta, E. G., and Hansford, R. G. (1999) PUFA and aging modulate cardiac mitochondrial membrane lipid composition and Ca2+ activation of PDH. *Am. J. Physiol.* **276**, H149–H158
206. Semba, R. D., Moaddel, R., Zhang, P., Ramsden, C. E., and Ferrucci, L. (2019) Tetra-linoleoyl cardiolipin depletion plays a major role in the pathogenesis of sarcopenia. *Med. Hypotheses.* **127**, 142–149
207. Löser, T., Joppe, A., Hamann, A., and Osiewacz, H. D. (2021) Mitochondrial phospholipid homeostasis is regulated by the i-AAA protease PaIAP and affects organismic aging. *Cells.* **10**, 2775
208. Zhou, J., Zhong, Q., Li, G., and Greenberg, M. L. (2009) Loss of cardiolipin leads to longevity defects that are alleviated by alterations in stress response signaling. *J. Biol. Chem.* **284**, 18106–18114
209. Sen, T., Sen, N., Tripathi, G., Chatterjee, U., and Chakrabarti, S. (2006) Lipid peroxidation associated cardiolipin loss and membrane depolarization in rat brain mitochondria. *Neurochem. Int.* **49**, 20–27
210. Paradies, G., Petrosillo, G., Paradies, V., and Ruggiero, F. M. (2010) Oxidative stress, mitochondrial bioenergetics, and cardiolipin in aging. *Free Radic. Biol. Med.* **48**, 1286–1295
211. Lee, H-J., Mayette, J., Rapoport, S. I., and Bazinet, R. P. (2006) Selective remodeling of cardiolipin fatty acids in the aged rat heart. *Lipids Health Dis.* **5**, 2
212. Marschall, L-M., Warnsmann, V., Meeßen, A. C., Löser, T., and Osiewacz, H. D. (2022) Lifespan extension of Podospora anserina mic60-subcomplex mutants depends on cardiolipin remodeling. *Int. J. Mol. Sci.* **23**, 4741
213. Ahmadpour, S. T., Mahéo, K., Servais, S., Brisson, L., and Dumas, J-F. (2020) Cardiolipin, the mitochondrial signature lipid: implication in cancer. *Int. J. Mol. Sci.* **21**, 8031
214. Kiebish, M. A., Han, X., Cheng, H., Chuang, J. H., and Seyfried, T. N. (2008) Cardiolipin and electron transport chain abnormalities in mouse brain tumor mitochondria: lipidomic evidence supporting the Warburg theory of cancer. *J. Lipid Res.* **49**, 2545–2556
215. Zhong, H., Xiao, M., Zarkovic, K., Zhu, M., Sa, R., Lu, J., *et al.* (2017) Mitochondrial control of apoptosis through modulation of cardiolipin oxidation in hepatocellular carcinoma: a novel link between oxidative stress and cancer. *Free Radic. Biol. Med.* **102**, 67–76
216. Dumas, J-F., Goupille, C., Julienne, C. M., Pinault, M., Chevalier, S., Bougnoux, P., *et al.* (2011) Efficiency of oxidative phosphorylation in liver mitochondria is decreased in a rat model of peritoneal carcinosis. *J. Hepatol.* **54**, 320–327
217. Zhang, J., Yu, W., Ryu, S. W., Lin, J., Buentello, G., Tibshirani, R., *et al.* (2016) Cardiolipins are biomarkers of mitochondria-rich thyroid oncocytic tumors. *Cancer Res.* **76**, 6588–6597
218. Zichri, S. B., Kolusheva, S., Shames, A. I., Schneiderman, E. A., Poggio, J. L., Stein, D. E., *et al.* (2021) Mitochondria membrane transformations in colon and prostate cancer and their biological implications. *Biochim. Biophys. Acta Biomembr.* **1863**, 183471
219. Morton, R., Cunningham, C., Jester, R., Waite, M., Miller, N., and Morris, H. P. (1976) Alteration of mitochondrial function and lipid composition in Morris 7777 hepatoma. *Cancer Res.* **36**, 3246–3254
220. Feo, F., Canuto, R. A., Bertone, G., Garcea, R., and Pani, P. (1973) Cholesterol and phospholipid composition of mitochondria and microsomes isolated from morris hepatoma 5123 and rat liver. *FEBS Lett.* **33**, 229–232
221. Garcea, R., Canuto, R. A., Gautero, B., Biocca, M., and Feo, F. (1980) Phospholipid composition of inner and outer mitochondrial membranes isolated from Yoshida hepatoma AH-130. *Cancer Lett.* **11**, 133–139
222. Zheng, L., Kelly, C. J., and Colgan, S. P. (2015) Physiologic hypoxia and oxygen homeostasis in the healthy intestine. A review in the theme: cellular responses to hypoxia. *Am. J. Physiol. Cell Physiol.* **309**, C350–C360
223. Young, R. M., Ackerman, D., Quinn, Z. L., Mancuso, A., Gruber, M., Liu, L., *et al.* (2013) Dysregulated mTORC1 renders cells critically dependent on desaturated lipids for survival under tumor-like stress. *Genes Dev.* **27**, 1115–1131
224. Ackerman, D., Tumanov, S., Qiu, B., Michalopoulou, E., Spata, M., Azzam, A., *et al.* (2018) Triglycerides promote lipid

homeostasis during hypoxic stress by balancing fatty acid saturation. *Cell Rep.* **24**, 2596–2605.e5
225. Reina-Campos, M., Heeg, M., Kennewick, K., Mathews, I. T., Galletti, G., Luna, V., *et al.* (2023) Metabolic programs of T cell tissue residency empower tumour immunity. *Nature.* **621**, 179–187
226. Kiebish, M. A., Han, X., Cheng, H., and Seyfried, T. N. (2009) In vitro growth environment produces lipidomic and electron transport chain abnormalities in mitochondria from non-tumorigenic astrocytes and brain tumours. *ASN Neuro.* **1**, AN20090011
227. Alsabeeh, N., Chausse, B., Kakimoto, P. A., Kowaltowski, A. J., and Shirihai, O. (2018) Cell culture models of fatty acid overload: problems and solutions. *Biochim. Biophys. Acta Mol. Cell Biol. Lipids.* **1863**, 143–151
228. Crabtree, H. G. (1929) Observations on the carbohydrate metabolism of tumours. *Biochem. J.* **23**, 536–545
229. Guppy, M., Greiner, E., and Brand, K. (1993) The role of the Crabtree effect and an endogenous fuel in the energy metabolism of resting and proliferating thymocytes. *Eur. J. Biochem.* **212**, 95–99
230. Rapport, M. M., and Franzl, R. E. (1957) The structure of plasmalogens. III. The nature and significance of the aldehydogenic linkage. *J. Neurochem.* **1**, 303–310
231. Norton, W. T., Gottfried, E. L., and Rapport, M. M. (1962) The structure of plasmalogens: VI. Configuration of the double bond in the α,β-unsaturated ether linkage of phosphatidal choline. *J. Lipid Res.* **3**, 456–459
232. Koivuniemi, A. (2017) The biophysical properties of plasmalogens originating from their unique molecular architecture. *FEBS Lett.* **591**, 2700–2713
233. Braverman, N. E., and Moser, A. B. (2012) Functions of plasmalogen lipids in health and disease. *Biochim. Biophys. Acta.* **1822**, 1442–1452
234. Nagan, N., and Zoeller, R. A. (2001) Plasmalogens: biosynthesis and functions. *Prog. Lipid Res.* **40**, 199–229
235. Werner, E. R., Keller, M. A., Sailer, S., Lackner, K., Koch, J., Hermann, M., *et al.* (2020) The TMEM189 gene encodes plasmanylethanolamine desaturase which introduces the characteristic vinyl ether double bond into plasmalogens. *Proc. Natl. Acad. Sci. U. S. A.* **117**, 7792–7798
236. Lee, R. G., Rudler, D. L., Raven, S. A., Peng, L., Chopin, A., Moh, E. S. X., *et al.* (2023) Quantitative subcellular reconstruction reveals a lipid mediated inter-organelle biogenesis network. *Nat. Cell Biol.* **26**, 57–71
237. Park, H., He, A., Tan, M., Johnson, J. M., Dean, J. M., Pietka, T. A., *et al.* (2019) Peroxisome-derived lipids regulate adipose thermogenesis by mediating cold-induced mitochondrial fission. *J. Clin. Invest.* **129**, 694–711
238. Brosche, T., and Platt, D. (1998) The biological significance of plasmalogens in defense against oxidative damage. *Exp. Gerontol.* **33**, 363–369
239. Cui, W., Liu, D., Gu, W., and Chu, B. (2021) Peroxisome-driven ether-linked phospholipids biosynthesis is essential for ferroptosis. *Cell Death Differ.* **28**, 2536–2551
240. Ginsberg, L., Rafique, S., Xuereb, J. H., Rapoport, S. I., and Gershfeld, N. L. (1995) Disease and anatomic specificity of ethanolamine plasmalogen deficiency in Alzheimer's disease brain. *Brain Res.* **698**, 223–226
241. Han, X., Holtzman, D. M., and McKeel, D. W., Jr. (2001) Plasmalogen deficiency in early Alzheimer's disease subjects and in animal models: molecular characterization using electrospray ionization mass spectrometry. *J. Neurochem.* **77**, 1168–1180
242. Lohner, K., Hermetter, A., and Paltauf, F. (1984) Phase behavior of ethanolamine plasmalogen. *Chem. Phys. Lipids.* **34**, 163–170
243. Han, X., and Gross, R. W. (1992) Nonmonotonic alterations in the fluorescence anisotropy of polar head group labeled fluorophores during the lamellar to hexagonal phase transition of phospholipids. *Biophys. J.* **63**, 309–316
244. Lohner, K. (1996) Is the high propensity of ethanolamine plasmalogens to form non-lamellar lipid structures manifested in the properties of biomembranes? *Chem. Phys. Lipids.* **81**, 167–184
245. Kaufman, A. E., Goldfine, H., Narayan, O., and Gruner, S. M. (1990) Physical studies on the membranes and lipids of plasmalogen-deficient Megasphaera elsdenii. *Chem. Phys. Lipids.* **55**, 41–48
246. Lohner, K. (1991) Effects of small organic molecules on phospholipid phase transitions. *Chem. Phys. Lipids.* **57**, 341–362
247. Kimura, T., Kimura, A. K., Ren, M., Berno, B., Xu, Y., Schlame, M., *et al.* (2018) Substantial decrease in plasmalogen in the heart associated with tafazzin deficiency. *Biochemistry.* **57**, 2162–2175
248. Kimura, T., Kimura, A. K., Ren, M., Monteiro, V., Xu, Y., Berno, B., *et al.* (2019) Plasmalogen loss caused by remodeling deficiency in mitochondria. *Life Sci. Alliance.* **2**, e201900348
249. Bozelli, J. C., Jr., Lu, D., Atilla-Gokcumen, G. E., and Epand, R. M. (2020) Promotion of plasmalogen biosynthesis reverse lipid changes in a Barth Syndrome cell model. *Biochim. Biophys. Acta Mol. Cell Biol. Lipids.* **1865**, 158677
250. van Meer, G., Voelker, D. R., and Feigenson, G. W. (2008) Membrane lipids: where they are and how they behave. *Nat. Rev. Mol. Cell Biol.* **9**, 112–124
251. Elustondo, P., Martin, L. A., and Karten, B. (2017) Mitochondrial cholesterol import. *Biochim. Biophys. Acta Mol. Cell Biol. Lipids.* **1862**, 90–101
252. Bosch, M., Marí, M., Herms, A., Fernández, A., Fajardo, A., Kassan, A., *et al.* (2011) Caveolin-1 deficiency causes cholesterol-dependent mitochondrial dysfunction and apoptotic susceptibility. *Curr. Biol.* **21**, 681–686
253. Martin, L. A., Kennedy, B. E., and Karten, B. (2016) Mitochondrial cholesterol: mechanisms of import and effects on mitochondrial function. *J. Bioenerg. Biomembr.* **48**, 137–151
254. Solsona-Vilarrasa, E., Fucho, R., Torres, S., Nuñez, S., Nuño-Lámbarri, N., Enrich, C., *et al.* (2019) Cholesterol enrichment in liver mitochondria impairs oxidative phosphorylation and disrupts the assembly of respiratory supercomplexes. *Redox Biol.* **24**, 101214
255. Torres, S., Solsona-Vilarrasa, E., Nuñez, S., Matías, N., Insausti-Urkia, N., Castro, F., *et al.* (2021) Acid ceramidase improves mitochondrial function and oxidative stress in Niemann-Pick type C disease by repressing STARD1 expression and mitochondrial cholesterol accumulation. *Redox Biol.* **45**, 102052
256. Kennedy, B. E., Madreiter, C. T., Vishnu, N., Malli, R., Graier, W. F., and Karten, B. (2014) Adaptations of energy metabolism associated with increased levels of mitochondrial cholesterol in Niemann-Pick type C1-deficient cells. *J. Biol. Chem.* **289**, 16278–16289
257. Cirigliano, A., Macone, A., Bianchi, M. M., Oliaro-Bosso, S., Balliano, G., Negri, R., *et al.* (2019) Ergosterol reduction impairs mitochondrial DNA maintenance in S. cerevisiae. *Biochim. Biophys. Acta Mol. Cell Biol. Lipids.* **1864**, 290–303
258. Helfrich, W. (1973) Elastic properties of lipid bilayers: theory and possible experiments. *Z. für Naturforschung C.* **28**, 693–703
259. Chakraborty, S., Doktorova, M., Molugu, T. R., Heberle, F. A., Scott, H. L., Dzikovski, B., *et al.* (2020) How cholesterol stiffens unsaturated lipid membranes. *Proc. Natl. Acad. Sci. U. S. A.* **117**, 21896–21905
260. Martinez, G. V., Dykstra, E. M., Lope-Piedrafita, S., and Brown, M. F. (2004) Lanosterol and cholesterol-induced variations in bilayer elasticity probed by 2H NMR relaxation. *Langmuir.* **20**, 1043–1046
261. Chen, Z., and Rand, R. P. (1997) The influence of cholesterol on phospholipid membrane curvature and bending elasticity. *Biophys. J.* **73**, 267–276
262. Cullis, P. R., and De Kruijff, B. (1978) Polymorphic phase behaviour of lipid mixtures as detected by 31P NMR. Evidence that cholesterol may destabilize bilayer structure in membrane systems containing phosphatidylethanolamine. *Biochim. Biophys. Acta.* **507**, 207–218
263. Tilcock, C. P. S., Hope, M. J., and Cullis, P. R. (1984) Influence of cholesterol esters of varying unsaturation on the polymorphic phase preferences of egg phosphatidylethanolamine. *Chem. Phys. Lipids.* **35**, 363–370
264. Beaven, A. H., Sapp, K., and Sodt, A. J. (2023) Simulated dynamic cholesterol redistribution favors membrane fusion pore constriction. *Biophys. J.* **122**, 2162–2175
265. Anderson, R. H., Sochacki, K. A., Vuppula, H., Scott, B. L., Bailey, E. M., Schultz, M. M., *et al.* (2021) Sterols lower energetic barriers of membrane bending and fission necessary

for efficient clathrin-mediated endocytosis. *Cell Rep.* **37**, 110008

266. Stepanyants, N., Macdonald, P. J., Francy, C. A., Mears, J. A., Qi, X., and Ramachandran, R. (2015) Cardiolipin's propensity for phase transition and its reorganization by dynamin-related protein 1 form a basis for mitochondrial membrane fission. *Mol. Biol. Cell.* **26**, 3104–3116

267. Barad, B. A., Medina, M., Fuentes, D., Wiseman, R. L., and Grotjahn, D. A. (2023) Quantifying organellar ultrastructure in cryo-electron tomography using a surface morphometrics pipeline. *J. Cell Biol.* **222**, e202204093

268. Garcia, G. C., Gupta, K., Bartol, T. M., Sejnowski, T. J., and Rangamani, P. (2023) Mitochondrial morphology governs ATP production rate. *J. Gen. Physiol.* **155**, e202213263